Commission of the European Community

JOINT
RESEARCH
CENTRE

NEANDC (E) 242 "U" Vol. III Euratom,
(INDC (EUR) 017/G).

ANNUAL PROGRESS REPORT ON NUCLEAR DATA

1982

CENTRAL BUREAU FOR NUCLEAR MEASUREMENTS

GEEL (BELGIUM)

March 1983

TABLE OF CONTENTS

NUCLEAR DATA

1. Neutron Data

A. Deruytter

1.1 CROSS SECTIONS OF ACTINIDES

Fission cross-section of ^{233}U and ^{241}Pu

C. Wagemans*, A. Deruytter, R. Barthélémy, J. Van Gils**

The $^{241}Pu(n,f)$ results were presented at the International Conference on Nuclear Data for Science and Technology (Antwerp, September 1982) with the following abstract:

" A series of measurements of the $^{241}Pu(n,f)$ reaction cross-section has been performed at GELINA. The neutron energy range from 10^{-2} eV up to 10^{5} eV was covered, allowing a normalization to the 2200 m/s reference cross-section. The neutron flux was determined via the $^{10}B(n,\alpha)^{7}Li$ reaction. Back-to-back ^{241}Pu-^{10}B foils were viewed by surface barrier detectors, so the fission fragments counting rate and the neutron flux were measured simultaneously and from the same position in the neutron beam. The present $\bar{\sigma}_f$-values are compared with previous results, giving special attention to the influence of the normalization. In particular, the situation of the secondary normalization integrals $\int_{12eV}^{20eV} \sigma_f dE$ and $\int_{0.1keV}^{1keV} \sigma_f dE$ is reviewed."

The $^{233}U(n,f)$ measurements were finalized and the data are being analysed.

Status of neutron capture data of ^{233}U, ^{235}U and ^{239}Pu in the unresolved resonance region

F. Corvi

An invited paper with this title was presented at the NEANDC/NEACRP Specialist's Meeting on Fast Neutron Capture Cross Sections, Argonne, 20-23 April 1982. The abstract reads as follows:

" First, the outstanding requests for σ_γ and α data of the three main fissile nuclei are briefly summarized. Then the methods employed in the last twenty years of differential α-measurements are critically

---

* SCK/CEN, Mol and R.U. Gent, Belgium

** SCK/CEN, Mol, Belgium

discussed. They can be classified into three groups: a) systems measuring simultaneously absorption radiation and fissions with two separate detectors; b) systems in which a large fraction of fission and capture γ-rays are identified by means of prompt or delayed coincidences with a high efficiency fission detection apparatus; c) systems consisting of a γ-ray detector only, in which capture and fissions are distinguished by some special feature of the radiation emitted. Advantages and drawbacks of the various techniques are discussed, particularly in connection with all sources of systematic errors. Measurements of alpha in the unresolved resonance region are separately reviewed for each of the three fissile isotopes."

Fission cross-section measurements at very low neutron energies

C. Wagemans*, A. Deruytter, E. Allaert, R. Barthélémy, J. Van Gils**

The feasibility of performing fission cross-section measurements in the sub-thermal neutron energy region is being investigated at GELINA. Test measurements were performed under various experimental conditions (linac repetition frequency, moderator thickness, detection geometry etc.), down to 1 meV neutron energy. Preliminary results for $\sigma_f(E)\sqrt{E}$ for ^{233}U in the neutron energy region from 1 meV up to 1.5 eV are shown in Fig. 1.1.

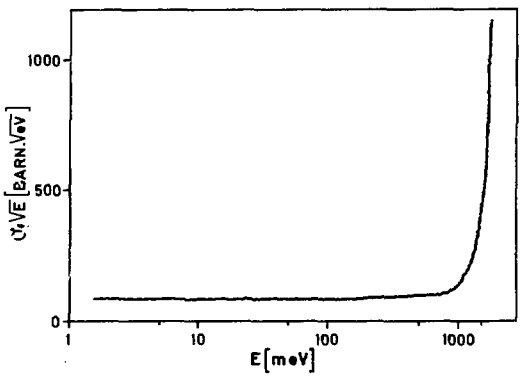

Fig. 1.1 $\sigma_f \sqrt{E}$ *for* $^{233}U(n,f)$

Measurement of neutron capture cross section and alpha of ^{235}U from 2 to 85 keV

F. Corvi, L. Calabretta***, M. Merla, T. van der Veen, M.S. Moore+

A paper with this title was presented at the NEANDC-NEACRP Specialist's Meeting on Fast Neutron Capture, Argonne, 20-23 April 1982. The paper had the following abstract:

---

* SCK/CEN, Mol and R.U. Gent, Belgium
** SCK/CEN, Mol, Belgium
*** Bursary of the European Community
+ Visiting Scientist from LANL

" A measurement of capture and alpha for ^{235}U was performed on a 28 m flight path at the Geel 150 MeV linac. The experimental set up consisted of a multiplate fission chamber surrounded by four C_6F_6 liquid scintillators each of 10.2 cm diameter and 7.5 cm height. The fission chamber itself was composed of 21 aluminium plates with back-to-back coatings of U_3O_8 enriched to 99.5 % ^{235}U with average thickness 1.16 mg/cm^2. The total ^{235}U content was 2.5 g. The efficiency of the chamber was separately measured in preliminary experiments. Pulses from C_6F_6 were first divided into two parts, depending whether in coincidence or not with fission chamber pulses, and then weighted according to their amplitude in order to achieve a response proportional to the total γ-ray energy. Background at 35 keV was monitored by keeping a 2.4 cm thick aluminium filter permanently in the beam. Its detailed shape was determined with a mock chamber run. Neutron flux was measured with a 0.5 mm thick ^6Li-glass. A separate run was performed with the fission chamber alone in order to deduce independent σ_f values. Capture data were then normalized to gold neutron capture as well as to thermal and resonance α-values. The different calibrations were found to agree within 3 %. Finally, average values of σ_f, σ_γ and α, together with their errors, were derived for neutron energies between 2 and 85 keV. It was found that, in the range 2 to 60 keV, the σ_γ values from the present work are on average about 10 % lower than the ENDF/B-V estimates."

Further assessment of ^{238}U resonance data with respect to p-wave resonance contamination of s-wave resonances

G. Rohr, R. Shelley, F. Poortmans*, E. Cornelis**, G. Vanpraet**

In previous papers [1,2] we have reported the parameters of resonances in ^{238}U, below 4.26 keV, obtained from transmission, capture and scattering measurements performed at the CBNM. The final resonance data listed in Table 2 of Ref. 2 includes only those Γ_γ values which are within three standard deviations of the mean value of (23.6 $\pm$ 0.11) meV. Values that did not fulfil this criterium had been assumed to be a doublet. As will be shown below, such an assumption was justified if we compare the resolution of our experiment with the average level spacing for p-wave resonances. In the present Table 1.1 all broad s-wave resonances for which we could determine the radiation widths are included. A pictorial representation is given in

(1) F. Poortmans, E. Cornelis, L. Mewissen, G. Rohr, R. Shelley, T. van der Veen, G. Vanpraet, H. Weigmann, Proc. Lowell Conf. (1976) page 1264

(2) F. Poortmans et al., The IAEA Consultants Meeting on Uranium and Plutonium Isotope Resonance Parameters, Vienna (1981), INDC(NDS)-129 GJ, p.112

* SCK/CEN, Mol, Belgium

** Rijksuniversitair Centrum, Antwerpen, Belgium

Table 1.1 The total radiative width for ^{238}U resonances

E (eV)	Γ_γ (meV)	E (eV)	Γ_γ (meV)	E (eV)	Γ_γ (meV)
6.67	24.2 ± 0.6	1405.90	25.6 ± 0.8	*2718.00	31. ± 1.
20.90	23.2 ± 0.6	1428.40	25.5 ± 1.0	2751.40	33. ± 2.
36.81	22.9 ± 0.3	1474.20	23.7 ± 0.6	2865.80	22.0 ± 1.4
66.06	24.0 ± 0.4	1523.00	23.6 ± 1.5	2883.50	24.6 ± 1.4
102.60	24.3 ± 0.4	1598.30	22.3 ± 0.7	2934.20	23.6 ± 1.5
116.88	22.8 ± 0.6	1623.10	22.5 ± 0.7	3004.40	24.9 ± 1.5
189.65	23.1 ± 0.7	1638.60	23.2 ± 0.7	3029.10	30. ± 2.
208.48	23.7 ± 0.7	1662.90	24.2 ± 0.8	3060.30	24.0 ± 3.0
237.34	25.0 ± 0.6	1689.30	23.8 ± 0.7	3110.20	50. ± 5.
273.62	22.5 ± 0.6	*1710.30	28.8 ± 1.8	3149.40	23.2 ± 1.4
290.97	22.6 ± 0.6	1723.30	22.1 ± 2.0	3179.50	29. ± 2.
347.71	22.7 ± 0.3	*1756.40	27.2 ± 1.	3189.40	21.5 ± 2.0
410.12	24.4 ± 0.6	1782.90	44.0 ± 5.	3206.40	27. ± 3.
433.91	23.5 ± 0.6	1808.80	25.0 ± 2.	3249.50	22.5 ± 2.5
463.07	23.5 ± 1.2	1903.30	25.0 ± 1.0	*3280.20	24.5 ± 1.5
518.54	23.4 ± 0.6	1917.60	23.5 ± 1.5	3313.00	27. ± 1.5
535.44	23.8 ± 0.3	*1969.60	30.5 ± 3.	3322.70	22.3 ± 2.0
580.30	25.0 ± 0.5	1974.90	26.5 ± 1.	3334.50	23.9 ± 1.8
595.21	23.2 ± 0.3	2024.10	23.7 ± 1.0	3356.60	23.6 ± 1.5
620.17	23.4 ± 0.4	2031.00	25.1 ± 1.2	*3409.50	26. ± 2.
661.30	24.3 ± 0.4	2146.10	24.2 ± 1.1	3536.90	23.9 ± 1.5
693.24	23.5 ± 0.5	2153.30	24.3 ± 0.8	3458.70	24.8 ± 2.0
708.49	23.3 ± 0.6	2187.00	24.1 ± 1.0	*3486.20	27. ± 1.
821.74	22.5 ± 0.6	2201.90	29.5 ± 1.7	3562.50	24.5 ± 2.
851.19	24.0 ± 1.0	2260.30	25.4 ± 1.5	3574.70	23. ± 3.
856.25	23.5 ± 1.0	2266.70	32. ± 2.	3630.60	29.5 ± 2.
* 905.25	25.0 ± 1.1	2282.40	28. ± 2.	*3693.70	28.4 ± 1.
* 925.34	24.8 ± 0.5	2354.00	32. ± 2.	3717.70	39. ± 4.
937.21	23.5 ± 0.7	2356.50	24.5 ± 1.5	3734.80	25.4 ± 1.5
958.65	23.5 ± 1.0	2392.60	28.5 ± 2.	3765.80	27. ± 2.5
* 991.65	24.7 ± 0.5	2427.60	26. ± 0.5	3782.50	24.0 ± 2.2
1054.80	22.8 ± 0.5	2447.20	23.5 ± 1.2	*3858.80	28.3 ± 1.5
1109.50	27.5 ± 1.5	2489.70	24.5 ± 1.3	3873.30	36. ± 2.
1140.70	23.8 ± 0.8	*2548.30	29.5 ± 1.	3902.90	24.3 ± 2.5
1168.00	24.2 ± 0.5	*2559.90	27.2 ± 1.0	3915.40	22.4 ± 2.5
*1177.40	31. ± 1.6	*2581.80	25.8 ± 1.0	3940.50	23.9 ± 2.5
*1195.30	25.5 ± 1.6	2598.00	22.5 ± 1.1	3955.70	28.5 ± 2.5
1245.40	22.5 ± 0.8	2620.50	26.5 ± 1.2	4064.70	25. ± 3.
1267.50	25.3 ± 1.4	*2633.60		4125.90	50. ± 5.
1273.50	22.4 ± 1.3	2672.70	24.0 ± 1.4	*4167.50	34.5 ± 3.
1394.40	24.0 ± 0.8	2697.10	26. ± 2.2	*4260.30	35. ± 4.

* Shape of cross section indicates doublet

Fig. 1.2 from which it can easily be seen, below 1 keV that the Γ_γ values fluctuate around the above mentioned mean value, whereas at higher energies the number of resonances with higher Γ_γ-values increases with energy. This is shown quantitatively in Fig. 1.3 where the number of these levels per energy bin of 500 eV is plotted as a function of the neutron energy (lower curve). The upper histogram represents the total number of resonances

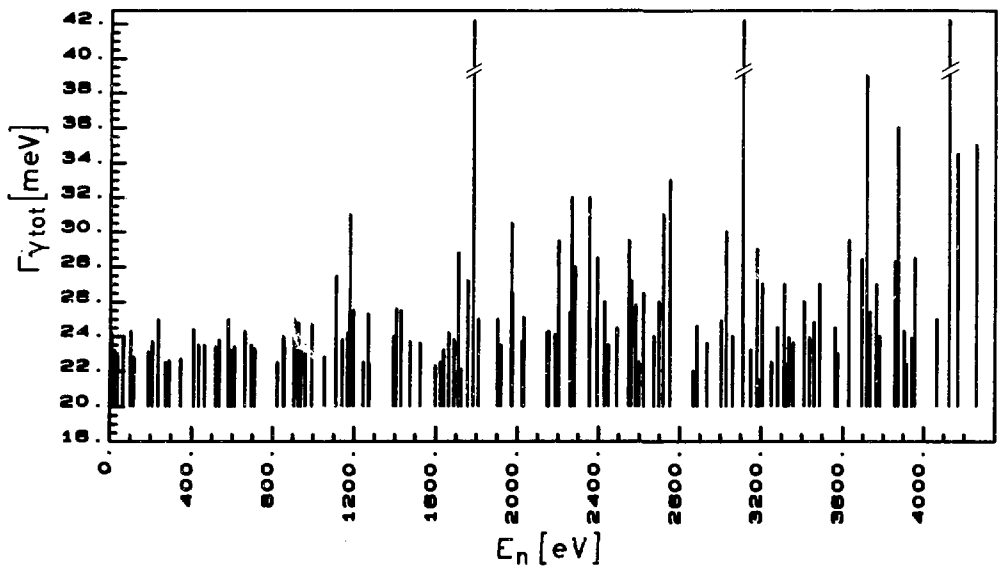

Fig. 1.2 The total radiative width as a function of neutron energy

with a known Γ_γ-value within the same energy bin. An explanation can be that small, undetected p-wave resonances contribute to the capture area of the broad s-wave resonances. Considering that the s-wave resonance width ΔE is composed of the Doppler width σ_D and the resolution width σ_{RW}, then the energy range covered by N resonances is N ΔE which for the first energy region of 500 eV, containing 15 resonances, yields 8.6 eV when ΔE = 0.57 eV.

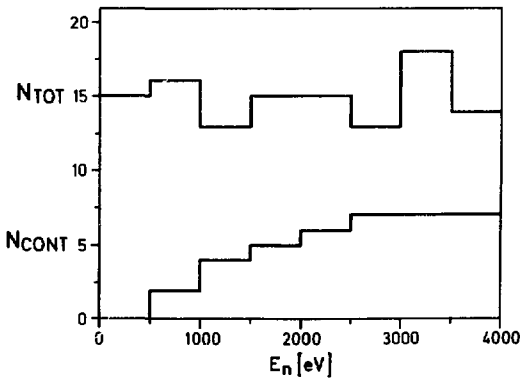

Fig. 1.3 The number of Γ_γ-values determined per energy bin of 500 eV plotted against neutron energy

An estimation of the number of contaminated s-wave resonances can be performed as follows:

If we assume an average level spacing D for p-wave resonances to be 1/3 of the level spacing D_0 for s-wave resonances, we obtain 7.2 eV and the number

of possibly screened p-wave resonances is 8.6/7.2 = 1.2, which can correspond to one contaminated s-wave resonance (N_{CONT}). For the other energy bins estimates are given in Table 1.2. They should be considered as lower limit values, since the energy range covered by s-wave resonances is based only on s-wave resonances, where Γ_γ has been determined.

Table 1.2 Estimation of s-wave resonances contaminated by p-waves

E^* (eV)	σ_D (eV)	σ_{RW} (eV)	ΔE(FWHM) (eV)	Nx ΔE (eV)	N_{CONT}
250	0.23	0.05	0.57	8.6	1.2
750	0.40	0.17	1.01	16.2	2.3
1250	0.51	0.29	1.39	18.1	2.5
1750	0.61	0.43	1.77	26.6	3.7
2250	0.69	0.57	2.10	31.5	4.4
2750	0.76	0.71	2.45	31.9	4.4
3250	0.83	0.87	2.83	50.9	7.0
3750	0.89	1.03	3.20	44.8	6.2

* *Energy of bin centre*

The results are in good agreement with those shown in the lower histogram of Fig. 1.3. Below 1 keV this effect is reduced due to the angular momentum barrier for p-wave resonances.

As shown, with increasing energy, the contamination of broad s-wave resonances does not permit an accurate determination of the total radiative width. The Γ_γ can become twice the mean value, if broad resonances of similar neutron width overlap [1]. Determining uncontaminated resonances by simply rejecting those with a Γ_γ value larger than 3 standard deviations of the mean is somewhat arbitrary. Therefore the mean value has been calculated using all 26 resonances below 900 eV, assuming a Gaussian distribution for the total radiative width. We get for the mean radiative width: $\Gamma_\gamma = (23.54 \pm 0.11)$ meV and the standard deviation of the radiation width frequency function is $\sigma_N = (0.689 \pm 0.117)$ meV, corresponding to an effective degree of freedom in the capture process of $\nu = 2334 \,^{+\,1053}_{-\,630}$.

---

(1) M.C. Moxon, M.G. Sowerby, AERE-R 10597 (1982)

These values have been reproduced by statistical model calculations using experimental data obtained from γ-ray spectra measurements together with the Fermi-gas formula for the level density and the giant dipole approximation for the energy transition law [1].

The degree of freedom has some relevance concerning the formalism to describe the shape of capture cross sections in resonances. In the usual Reich-Moore formalism the large number of capture channels has been eliminated from the R-matrix, by assuming that the capture amplitudes have random sign and size variations for the various channels, so that the level-level interference in capture does not play a role. The accuracy of this approximation depends on the number of effective degrees of freedom in the capture process and has been studied in Ref. [2] by comparing the envelope of resonances calculated with different R-matrix predictions. According to this, the high degree of freedom deduced from Uranium data guarantees that the shape of capture resonances, including tails, can be accurately described by the Reich-Moore formalism.

Fission cross section of ^{238}Pu

C. Budtz-Jørgensen, H.-H. Knitter, D.L. Smith*, H. Bax, R. Vogt

The evaluation of the measurements, which cover a neutron energy range from 5 eV to 10 MeV was completed. A paper "Neutron Induced Fission Cross Section of ^{238}Pu in the Energy Range from 5eV to 10 MeV" was prepared and presented at the International Conference on Nuclear Data for Science and Technology (Antwerp, September 1982). The abstract is:

" The fission cross section of ^{238}Pu was measured in the neutron energy range from 5 eV to 10 MeV. Several methods of neutron production were employed using the Van de Graaff and the electron linear accelerator of the CBNM. The neutron induced fission events were detected with a specially designed ionization chamber that permitted discrimination against the high α-activity of the ^{238}Pu sample. The fission cross section was measured relative to the ^{235}U(n,f) cross section above 100 keV and at lower neutron energies relative to the ^{6}Li(n,t)^{4}He cross section shape, however normalized between 7.8 eV and 11.0 eV to the known resonance fission integral of ^{235}U.
The present data provide unique new information above 5 MeV covering the second chance fission threshold. In the resonance region the existence of intermediate structures as observed in a previous nuclear explosion measurement was confirmed".

---

(1) G. Rohr, Neutron Capture Gamma-Ray Spectroscopy, Brookhaven, 1978, p. 734

(2) S.H. Kim, D.R. Harris, R.C. Block, Neutron Physics and Nuclear Data, Harwell (1978) p. 730

* Visiting Scientist from ANL

The main results of this work are shown in Figs. 1.4 and 1.5.

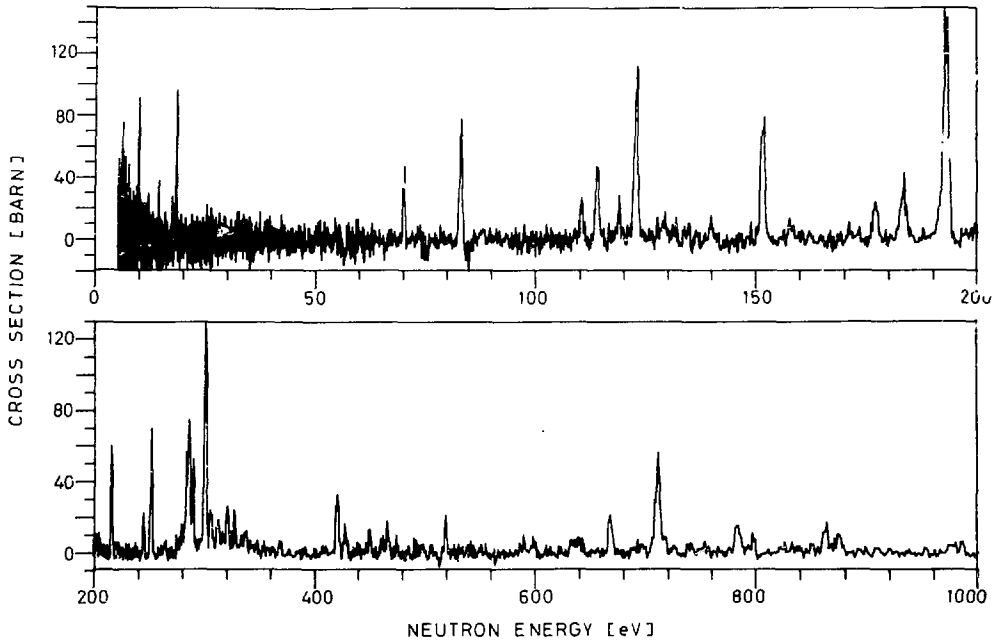

Fig. 1.4 Neutron-induced fission cross section of ^{238}Pu from 5 eV to 1 keV

Fission fragment mass and energy distribution for the thermal neutron induced fission of ^{239}Pu and the spontaneous fission of ^{240}Pu

E. Allaert, C. Wagemans*, A. Deruytter, P. Schillebeeckx*, R. Barthélémy

The characteristics of the energy and mass distributions of the ^{240}Pu(s.f.) fragments are a controversial problem in the fission physics field. Indeed, since 1958 seven comparative measurements of the $^{239}Pu(n_{th},f)$ and the ^{240}Pu(s.f.) reactions have been performed yielding quite discrepant results for both the energy and the mass characteristics. Taking profit of the improved experimental conditions (on-line data reduction, high quality targets), we started a re-investigation of this problem. A first experiment is being performed at an 8 m flight-path of GELINA, using a mixed ^{239}Pu-^{240}Pu layer (25 % ^{239}Pu, 75 % ^{240}Pu; thickness 57 $\mu g/cm^2$) evaporated onto a 30 $\mu g/cm^2$ polyimide backing. Partial results indicate that the fissioning

* SCK/CEN, Mol and R.U. Gent, Belgium

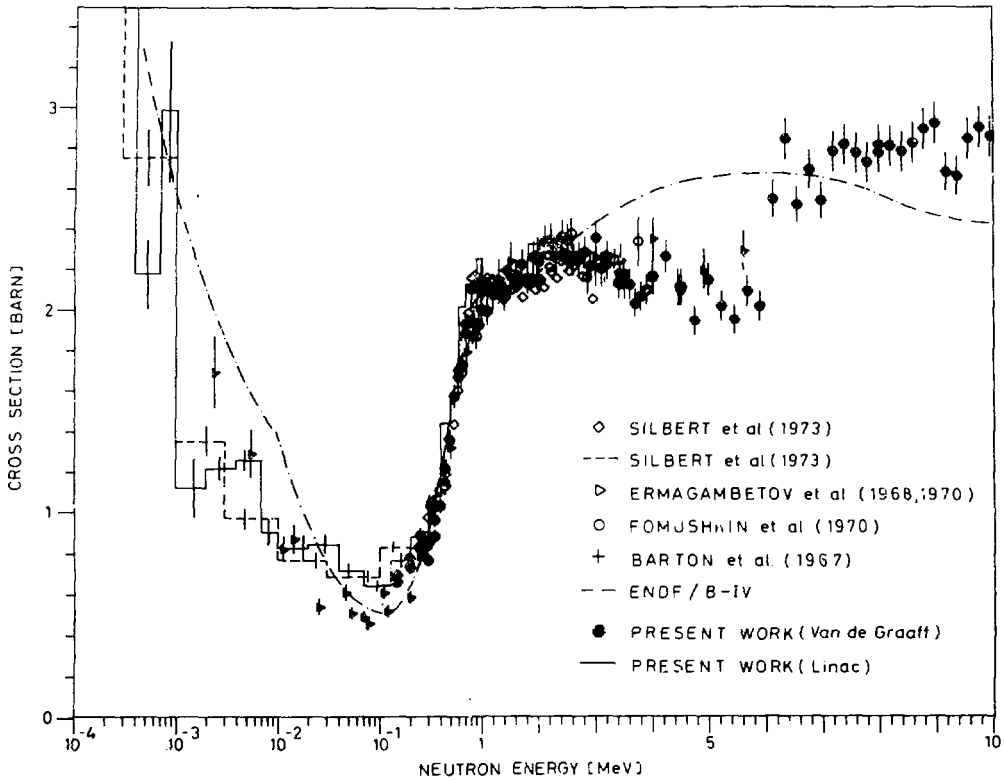

Fig. 1.5 Neutron-induced fission cross section of ^{238}Pu from 400 eV to 10 MeV. Note that the energy scale is logarithmic below 1 MeV and linear above

system ^{240}Pu behaves in a very similar way as ^{242}Pu, i.e. a higher average total kinetic energy for ^{240}Pu(s.f.) than for $^{239}Pu(n_{th},f)$, a much higher peak yield, more pronounced fine structures and a narrower mass-distribution for the spontaneous fission than for the neutron induced fission. These measurements are being continued.

Fission fragment mass- and energy distributions for the thermal neutron induced fission of ^{241}Pu and the spontaneous fission of ^{242}Pu and ^{244}Pu

E. Allaert*, C. Wagemans*, G. Wegener-Penning**, A. Deruytter, R. Barthélémy

The measurements as well as the analysis have been completed. These results were at the basis of the Dr.Sc. thesis of E. Allaert which has been submitted

* SCK/CEN, Mol and R.U. Gent, Belgium
** SCK/CEN, Mol, Belgium

Table 1.3 Main characteristics of the $^{241}Pu(n_{th},f)$, $^{242}Pu(s.f.)$ and $^{244}Pu(s.f.)$ fragment mass- and energy-distributions. The errors are only statistical.

	$^{241}Pu(n_{th},f)$	$^{242}Pu(s.f.)$	$^{244}Pu(s.f.)$
$\bar{E}_K$ (MeV)	176.56 ± 0.07	180.03 ± 0.09	182 ± 1 a)
$\bar{E}_K^*$ (MeV)	178.97 ± 0.07	181.78 ± 0.09	184 ± 1 a)
σ_{E_K} (MeV)	12.0	11.9	12.1
$\bar{E}_L^*$ (MeV)	103.10 ± 0.05	103.21 ± 0.06	103.7 ± 0.7 a)
$\bar{E}_H^*$ (MeV)	75.87 ± 0.05	78.57 ± 0.06	80.3 ± 0.7 a)
$\bar{m}_L^*$ (amu)	102.45 ± 0.04	104.50 ± 0.05	106.31 ± 0.08
$\sigma_{m_L^*}$ (amu)	6.72	5.82	6.45
$\bar{m}_H^*$ (amu)	139.55 ± 0.04	137.50 ± 0.05	137.69 ± 0.08
$\sigma_{m_H^*}$ (amu)	6.72	5.82	6.45
$\bar{m}_L$ (amu)	100.64 ± 0.04	103.12 ± 0.05	104.76 ± 0.08
σ_{m_L} (amu)	6.47	5.79	6.25
$\bar{m}_H$ (amu)	138.45 ± 0.04	136.77 ± 0.05	136.92 ± 0.08
σ_{m_H} (amu)	6.41	5.78	6.25
$\Delta\bar{E}_K^*$ (MeV)	25.0 ± 3.2	18.3 ± 4.7	19.3 ± 6.1
$\bar{\nu}_t$	2.927	2.10	2.30
N	3×10^4	1.8×10^4	6×10^3

a) Statistical error + error due to the energy loss corrections

to the Faculty of Sciences of the Gent University. A final report on this research has been accepted for publication in Nuclear Physics A with the following abstract:

" The energy and mass distributions and their correlations have been studied for the spontaneous fission of ^{242}Pu and ^{244}Pu and for the thermal-neutron induced fission of ^{241}Pu. A comparison of the ^{242}Pu(s.f.) and the ^{241}Pu(n_{th},f) results shows a narrower mass distribution, a much higher peak yield and a more pronounced fine structure for the spontaneous fission than for the neutron induced fission. The average total kinetic energy is higher for ^{242}Pu(s.f.) than for ^{241}Pu(n_{th},f), and also the energy-mass correlations behave differently in both cases. The ^{244}Pu(s.f.) data are very similar to these for ^{242}Pu(s.f.). All these results are discussed and interpreted in the frame of the scission point model of Wilkins et al. (Phys. Rev. 14 (1976) 1832)."

In Table 1.3 the main characteristics of the ^{241}Pu(n_{th},f), ^{242}Pu(s.f.) and ^{244}Pu(s.f.) fragment mass- and energy-distributions are summarized. Fig. 1.6 illustrates the similarity of the ^{242}Pu(s.f.) and the ^{244}Pu(s.f.) mass-distributions.

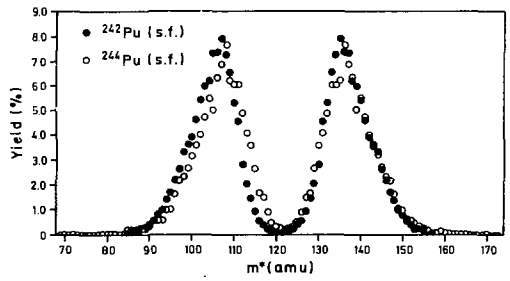

Fig. 1.6 The ^{242}Pu(s.f.) and ^{244}Pu(s.f.) fragment mass-distributions

Fission cross section of ^{242}Pu

J.A. Wartena, H. Weigmann, C. Bürkholz

The measurements on the neutron induced fission cross section of ^{242}Pu have been completed using neutron flight paths of 9 m and 25 m at the GELINA. The data obtained for high neutron energies (0.3 MeV $\leq E_n \leq$ 10 MeV) have been analysed. The neutron flux was determined from the ^{235}U(n,f) reaction rate using the ENDF/B-V cross section data. Fig. 1.7 shows the resultant cross section.

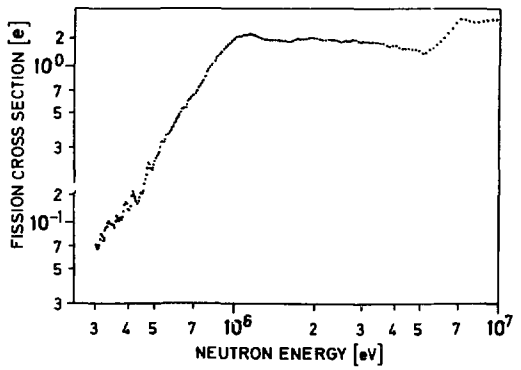

Fig. 1.7 Measured fission cross section of ^{242}Pu

The systematic uncertainty common to all data points is ± 3 %.
Table 1.4 lists the ^{242}Pu fission cross section averaged over a number of broad energy intervals.

Table 1.4 Average ^{242}Pu fission cross section

Energy interval (MeV)	Cross section (b)	Statistical uncertainty (b)	Total uncertainty (b)
0.3 - 0.4	0.0985	0.0003	0.0030
0.4 - 0.5	0.1772	0.0004	0.0053
0.5 - 0.6	0.3425	0.0007	0.010
0.6 - 0.7	0.5503	0.0011	0.017
0.7 - 0.8	0.7935	0.0017	0.024
0.8 - 1.0	1.243	0.0020	0.037
1. - 2.	1.490	0.0016	0.045
2. - 3.	1.445	0.0030	0.043
3. - 4.	1.377	0.0042	0.042
4. - 5.	1.280	0.0056	0.039
5. - 6.	1.282	0.0088	0.039
6. - 7.	1.677	0.014	0.052
7. - 8.	1.920	0.021	0.061
8. - 10.	1.936	0.024	0.063

At lower energies (E_n < 0.3 MeV) the fission cross section of ^{242}Pu shows a large amount of structure. Analysis of the data in this energy region has been started.

Sub-barrier fission of ^{244}Pu

M.S. Moore*, J.A. Wartena, H. Weigmann, C. Budtz-Jørgensen, H.-H. Knitter

Below 100 keV neutron energy the measured fission cross section of ^{244}Pu shows a number of isolated peaks (see PPR July-December 1981). They are interpreted as being due to individual class II levels with their fission strength being spread over a very small number, often only one, of class I levels. In order to support this interpretation, a Monte Carlo simulation has been performed, in which ladders of class I and class II levels and

---

* Visiting Scientist from LANL

coupling parameters are sampled from the relevant distribution laws. The result of this simulation consists in a verification of the above interpretation, and in an estimate of the fission barrier parameters required to explain the observed structure.

1.2 CROSS SECTIONS OF STRUCTURAL MATERIALS

^{54}Fe neutron capture cross section

A. Brusegan, F. Corvi, G. Rohr, R. Shelley, T. van der Veen,
C. Van der Vorst, B.J. Allen*

This measurement has been performed at the GELINA on a 97.69 % enriched ^{54}Fe oxide sample (on loan from ORNL) (9.92 10^{-3} nuclei/b thick) in the range from 0.3 to 500 keV neutron energy and with a nominal resolution of 0.086 μs/m. The detecting system consisted of a pair of 4" x 3" C_6D_6 liquid scintillators viewing either the ^{54}Fe sample or the 0.3 cm thick $^{10}B_4C$ slab, used for the neutron flux determination. A 0.35 cm thick carbon scatterer replaced the $^{10}B_4C$ slab for the background measurement in the case of the flux determination. The ^{54}Fe capture data have been normalized to the transmission results for the 1.15 keV resonance of ^{56}Fe (Γ_n = (58.9 $\pm$ 2.0).10^{-3} eV, Γ_γ = (0.610 $\pm$ 0.060) eV). This latter isotope is present as a 2.25 % impurity in the sample.

Modified versions of the area code TACASI [1] and of the shape analysis code FANAC [2] have been applied to deduce from the measured capture cross section yields the resonance parameters and the capture areas ($g\Gamma_n\Gamma_\gamma/\Gamma$) listed in Table 1.5 together with those of Allen et al. [3].

The neutron widths for the known s-wave resonances are taken from the work of Cornelis et al. [4] except for the 7.8 keV and for the $g\Gamma_n$ values of the non s-wave resonances quoted by Pandey et al. [5].

---

(1) F.H. Fröhner, 1966, Report GA-6096

(2) F.H. Fröhner, 1976, Report KFK 2129

(3) B.J. Allen, A.R. de L. Musgrove, J.W. Boldeman, R.L. Macklin, AAEC/E403, (1977) and Proc. Spec. Meeting, CBNM, Geel, 1977, p. 447

(4) E.M. Cornelis, C.R. Jungmann, L. Mewissen, F. Poortmans, Proc. Int. Conf. on Nuclear Cross Section for Technology, Knoxville, 1979, p. 159

(5) M.S. Pandey, J.B. Gary, Proc. Int. Conf. on Nuclear Cross Section and Technology, Washington, D.C., 1975, p. 748

* AAEC - Australian Atomic Energy Commission Research Establishment, Lucas Heights Research Laboratories, Sutherland, NSW 2232, Australia

Table 1.5 Capture areas and resonance parameters of ^{54}Fe in the range 1 to 200 keV from the present work compared to the results of ORNL-AAEC [3]

PRESENT RESULTS						ORNL-AAEC RESULTS [b]
E_o (keV)	$\bar{w}$	$g\Gamma_n\Gamma_\gamma/\Gamma$ (eV)	$g\Gamma_n$ (eV)	$g\Gamma_\gamma$ (eV)	J^π	$g\Gamma_n\Gamma_\gamma/\Gamma$ (eV)
3.099	23.	0.0028 ± 0.0003				0.0030
7.80	44.	1.74 ± 0.11	1040. ± 100.	1.74 ± 0.11	$1/2^+$	1.8 ± 0.4
9.486	30.	0.55 ± 0.03	1.2 ± 0.3	1.03 ± 0.10		0.55
11.181	40.	0.77 ± 0.04	7.7 ± 0.8	0.86 ± 0.05		0.69
13.581	31.	0.035 ± 0.003				0.034
14.465	30.	0.62 ± 0.02	1.4 ± 0.5	1.12 ± 0.07		0.62
19.278	31.	0.050 ± 0.004				0.047
23.03	32.	0.37 ± 0.02				0.39
28.22	32.	0.16 ± 0.01				0.17
30.66	29.	0.83 ± 0.03	7.7 ± 1.0	0.93 ± 0.04		0.96
35.26	27.	0.23 ± 0.02				0.26
38.44	28.	0.83 ± 0.03				0.92
39.14	29.	0.77 ± 0.04	17. ± 2.	0.81 ± 0.04		0.82
41.20	31.	0.024 ± 0.006				0.028
50.14	29.	0.056 ± 0.07				0.075
51.58	35.	0.36 ± 0.03	6. ± 2.	0.38 ± 0.04		0.36
52.84	41.	1.50 ± 0.30	1978. ± 1.	1.50 ± 0.30	$1/2^+$	2.4 ± 0.4
53.59	24.	0.52 ± 0.04	17. ± 3.	0.54 ± 0.04		0.50
55.07	29.	0.62 ± 0.05				0.68
55.43	29.	0.55 ± 0.05	32. ± 3.	0.56 ± 0.05		0.68
59.20	29.	0.37 ± 0.03				
68.76	25.	0.24 ± 0.03				0.31
71.81	26.	0.28 ± 0.15	1676. ± 1.	0.28 ± 0.15	$1/2^+$	1.32 ± 0.26
75.80	29.	0.65 ± 0.03				0.76
77.21	27.	1.29 ± 0.06	4. ± 2.	1.91 ± 0.14		1.62
81.28	38.	0.29 ± 0.03				0.30 ± 0.03
83.19	26.	0.96 ± 0.07				1.27
83.48	30.	0.36 ± 0.05				0.45 ± 0.03
87.33	32.	0.39 ± 0.04				0.50
91.67	28.	0.25 ± 0.03				
97.77	35.	0.11 ± 0.02				0.24 ± 0.03
98.80	48	1.20 ± 0.25	511. ± 5.	1.20 ± 0.25	$1/2^+$	1.65 ± 0.25
99.84	24.	0.73 ± 0.06				0.79
101.71	21.	0.29 ± 0.03				0.35 ± 0.02
104.18	24.	0.60 ± 0.06				0.79
112.63	28.	0.64 ± 0.07				0.72
112.96	30.	0.42 ± 0.06				0.56
115.85	31.	1.06 ± 0.07	26. ± 5.	1.10 ± 0.07		1.21
119.78	49.	1.01 ± 0.09	26. ± 8.	1.05 ± 0.10		1.11
120.81 [a]	25.	0.72 ± 0.11	40. ± 10.	0.73 ± 0.11		0.89
126.4 [a]	29.	2.5 ± 0.4	60. ± 10.			2.59
127.15	36.	0.12 ± 0.04				
130.00	40.	2.9 ± 0.9	3470. ± 10.	2.9 ± 0.9	$1/2^+$	3.22 ± 0.64
135.81	31.	0.50 ± 0.05	80. ± 10.	0.50 ± 0.05		0.69
137.93	37.	0.61 ± 0.05				0.96
141.01	25.	0.59 ± 0.07				0.48
142.82	25.	1.30 ± 0.12				1.72
145.51	30.	0.48 ± 0.07				0.56
147.49	37.	0.54 ± 0.49	3780. ± 15.	0.54 ± 0.49	$1/2^+$	2.31 ± 0.46
150.47	43.	2.10 ± 0.17				2.88
152.71	27.	1.28 ± 0.15				1.78
153.22	25.	0.92 ± 0.11	60. ± 10.	0.93 ± 0.12		1.14
157.18	33.	1.06 ± 0.10				1.45
159.29	40.	1.39 ± 0.17	100. ± 10.	1.41 ± 0.17		1.89
164.64	35.	3.56 ± 0.25	105. ± 10.	3.59 ± 0.27		4.12
165.33	26.	0.87 ± 0.14	75. ± 10.	0.88 ± 0.14		0.81
174.07	32.	0.79 ± 0.16				0.82
174.09		0.58 ± 0.72	4590. ± 30.	0.58 ± 0.72	$1/2^+$	3.5 ± 1.1
177.94	37.	1.70 ± 0.20				1.88
182.38	28.	1.02 ± 0.16	150. ± 15.	1.03 ± 0.16		1.20
188.00		< 0.9	38170. ± 100.	< 0.9	$1/2^+$	10.0 ± 4.0
189.09	28.	0.27 ± 0.09				0.49 ± 0.03
192.12	31.	1.07 ± 0.14				1.33
194.05	45.	1.03 ± 0.20				1.14
194.56	39.	1.67 ± 0.21	100. ± 15.	1.70 ± 0.22		1.69
197.70	26.	0.85 ± 0.13				1.23

a) Doublet
b) Statistical and background errors are less than 5 % unless the error is quoted

In Fig. 1.8 the measured capture yield and the shape analysis fit to the data are shown for the energy range from 90 keV to 180 keV.

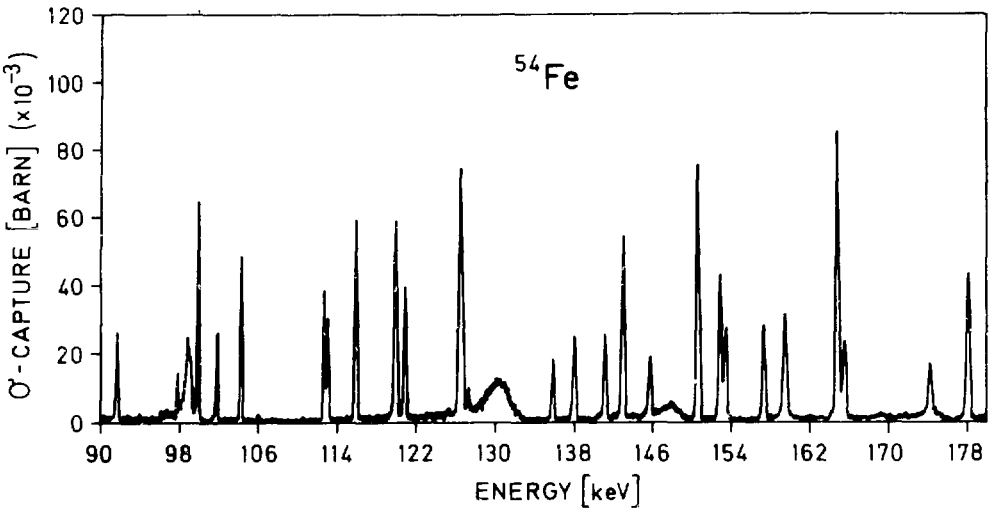

Fig. 1.8 The ^{54}Fe "capture cross section" vs neutron energy from 90 to 180 keV

For non s-wave resonances and for a selected set, the present capture areas compare well with those of our first ^{54}Fe run [1], partly published in ref. [2]: the ratio of the two sets is 1.04 on average. For the same set of resonances our results are lower than those of ORNL (see Ref. 3, page 15), the deviation is on average 4 % below 30 keV and 17 % at higher energy. Our results for s-wave resonances include a neutron sensitivity correction (prompt background correction) which is directly proportional to the neutron scattering widths of the resonances. The prompt background uncorrected s-wave capture widths show a good agreement with those published at Grenoble below 130 keV. At higher energy a large deviation is observed: this is due to the sensitivity of the results to the background determination (a 40 % reduction for the uncorrected Γ_γ of the 188 keV can be produced by a change of only 4 % in the background).

---

(1) A. Brusegan, F. Corvi, G. Rohr, R. Shelley, T. van der Veen, B.J. Allen, Proc. Int. Conf. on Neutron-Capture Gamma-Ray Spectroscopy and Related Topics, Grenoble, 7-11 September 1981, p. 408

(2) G. Rohr, Proc. Spec. Meeting on Fast Neutron Capture Cross Sections, Argonne, 1982

In general for s-wave resonances the present results confirm the conclusion drawn in our previous work (see Ref. 1, page 17) and show how doubtful is a prove of valence neutron effects in ^{54}Fe deduced from correlation studies (see Ref. 3, page 15).

High resolution neutron capture measurements of ^{56}Fe

F. Corvi, A. Brusegan, R. Buyl, G. Rohr, R. Shelley, T. van der Veen

The data normalization adopted was still the same as that used in our preliminary paper, that means it was based on the value $\Gamma_n = 58 \pm 3$ meV for the neutron width of the 1.15 keV resonance or equivalently a value $g\Gamma_n\Gamma_\gamma/\Gamma = 53 \pm 3$ meV for its capture area.
Such a value was deduced from a transmission measurement on a 2 mm thick metallic sample and was recently confirmed by a measurement on a 1 mm thick sample.
To check this normalization, we have carried out accurate calibrations of Fe capture relative to Ag and Au capture rates at both thermal and resonance energies. The results are summarized in Table 1.6.

Table 1.6 Results of calibration tests of capture in natural and enriched Fe samples relative to capture in Ag and Au at thermal and resonance energies

Calibration Energy	Calibration Element	Sample Thickness	Fe Sample Nucl. Thickness	R(reference value)	C (value from calibrations)	ϵ = C/R
E_{th} = 0.025 eV	Au	0.1 mm	Fe 0.5, 1 mm	σ_{th} = 2.56 ± .03 b	σ_{th} = 2.82 ± .08 b	1.10 ± .04
E_{th} = 0.025 eV	Au	0.1 mm	^{56}Fe 0.5 mm	σ_{th} = 2.59 ± .14 b	σ_{th} = 2.79 ± .08 b	1.08 ± .07
E_o = 4.9 eV	Au	0.1 mm	^{56}Fe 0.5 mm	A_γ = 53 ± 3 meV	A_γ = 66.2 ± 2.8 meV	1.25 ± .09
E_o = 5.2 eV	Ag	0.2 mm				

At thermal energy both natural and enriched Fe samples (on loan from ORNL) were compared to the Au standard. The saturated resonance technique was applied in the epithermal region, making use of the Ag and Au resonances at 5.2 and 4.9 eV, respectively: the two normalization constants obtained differed by 2.8 % and their average was taken. After correcting for the relative neutron flux, measured always with a ^6Li glass, a value $A_\gamma = g\Gamma_n\Gamma_\gamma/\Gamma = 66.2 \pm 2.8$ meV was derived for the 1.15 keV resonance, corresponding to $\Gamma_n = 74.3 \pm 3$ meV. Such a capture area is 25 % larger than the value

obtained from transmission and listed under R in Table 1.6. A similar trend is apparent at thermal energy though here the effect is limited to 8 - 10 %. This difference of the relative efficiency ϵ between thermal and resonance energies is really not to be understood since the γ-ray spectrum of the 1.15 keV resonance is very similar to the thermal one.

The data were analysed both with the modified area programme TACASI and with the R-matrix shape fitting code FANAC. For each resonance, the value of J, l, and Γ_n or Γ_γ (which ever was the larger) from the evaluation of F. Perey et al.[1] were taken as fixed input parameters in the codes. The values of Γ_γ or Γ_n (which ever was the lower) and consequently of the capture areas $g\Gamma_n\Gamma_\gamma/\Gamma$ were obtained for each of the 79 resonances analysed in the range from 1 to 256 keV. The average radiation widths, their standard deviations and the related effective number of degrees of freedom for different l values were found to be:

$$<\Gamma_\gamma> = 0.85 \pm 0.41 \ (\nu_{eff} = 9.6) \quad \text{for s-waves}$$
$$<\Gamma_\gamma> = 0.50 \pm 0.18 \ (\nu_{eff} = 17.1) \quad \text{for p-waves}$$
$$<\Gamma_\gamma> = 0.73 \pm 0.25 \ (\nu_{eff} = 18.5) \quad \text{for d-waves}$$

These values compare well with the results of the statistical model calculation reported in Ref. [2].

The present values of Γ_γ for s-wave resonances are considerably smaller than the corresponding ORNL values. Moreover the capture areas for p- and d-waves are on average 11 % lower than those of F. Perey et al.(1). Since the ORNL data have been normalized to the Au standard, the sign of this discrepancy is in keeping with the results of the calibration tests of Table 1.6. Because of this discrepancy and more particularly of the unsettled situation of the normalization procedure, the case of ^{56}Fe data cannot be considered as settled. Moreover we are extending the analysis up to 350 keV.

^{57}Fe transmission measurements below 100 keV

A. Brusegan, G. Van der Vorst

The ^{57}Fe neutron total cross section has been measured at GELINA in the energy range 0.6 - 150 keV, at a 49 m flight path (see Fig. 1.9). The iron sample (on loan from ORNL) consisted of 66.1 g of Fe_2O_3 (37.6 g enriched at 90.42 % and 28.5 g at 93.38 %), yielding a total final thickness of $8.98 \cdot 10^{-3}$ at/b in ^{57}Fe.

(1) F. Perey et al., Neutron Data of Structural Materials for Fast Reactors, Geel 1977, Pergamon Press, p. 530

(2) G. Rohr, Neutron Capture Gamma-Ray Spectroscopy, Plenum Press, 1979, p. 734

Neutrons have been detected via the $^{10}B(n,\gamma)$ reaction on a 0.5 cm thick sintered boron slab, viewed by two 4" x 3" NaI(Tl) detectors. Resonance parameters have been determined with shape analysis programmes, i.e. SIOB and FANAC. The second one has been modified in order to correct the theoretical transmission for the different time widths adopted in the T.O.F. spectrum.

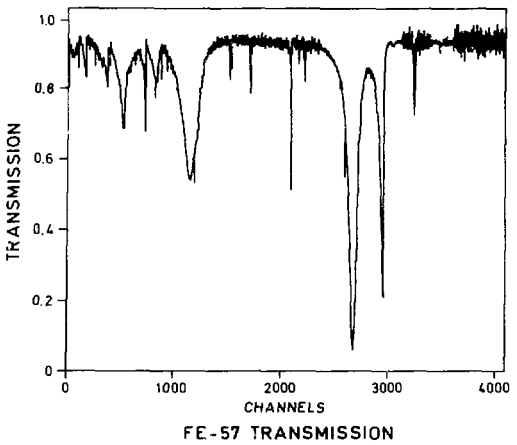

Fig. 1.9 ^{57}Fe *transmission*

For spin 1 s-wave resonances in ^{57}Fe, above 14.4 keV neutron energy, the inelastic scattering channel is open, the inelastic neutron widths being even orders of magnitude larger than the total capture widths: in such a case it is possible to deduce from the shape analysis of the spectra both the elastic and the inelastic neutron amplitudes. The preliminary results for s-wave resonances are systematically lower than those given by G. Rohr et al. [1]. In the energy range 52-72 keV the two s-wave resonances at about 56 and 61 keV can not amount for the measured transmission shape. The resonance at 13.9 keV has been identified as an s-wave with spin 1. The analysis of the p-wave resonances is underway. In the low neutron energy, the Γ_n of the 1.63 keV resonance is of particular interest in normalizing the capture yields for ^{57}Fe. It has been used in the study of the properties of the C_6D_6 detectors [2].

The status of structural material data in the resolved resonance region

G. Rohr

This contribution has been presented as an invited paper at the Specialist's Meeting on Fast-Neutron Capture Cross Sections (Argonne, April, 1982) with the following abstract:

---

(1) G. Rohr and K.N. Müller, Z. Physik 227 (1969) 1

(2) G. Rohr et al., Resonance Parameters of ^{57}Fe, International Conference on Nuclear Data for Science and Technology, Antwerp, 6-10 September 1982, Proceedings in press

" This review is mainly concerned with the accuracy aspect of neutron capture data for structural materials. As examples data sets of ^{54}Fe, ^{56}Fe and ^{57}Fe will be compared critically. The results of the investigation of the C_6D_6 detector performed at CBNM will be used to study the deviations in the different data sets. Recommendations to reduce the uncertainty of capture data and to improve the capture detectors using the weighting method will be given."

1.3 CROSS SECTIONS OF FISSION PRODUCTS

Average capture cross section of the fission product nuclei $^{104,105,106,108,110}Pd$

E. Cornelis*, C. Bastian, G. Rohr, R. Shelley, T. van der Veen, G. Vanpraet*

Neutron capture cross section measurements on enriched stable Pd isotopes (on loan from ORNL) have been performed at the 30 m time of flight station of GELINA in the energy range of 10 eV up to 600 keV. The neutron flux shape was monitored with a 0.5 mm ^{6}Li-glass scintillator and the relative neutron flux was measured with a 0.6 mm $^{10}B_4C$-slab. The time-dependent background was determined using the black resonance technique as well as the yield from a 0.5 mm ^{208}Pb capture sample. Experimental data normalization was obtained by using resonance parameters of low energy resonances in ^{105}Pd, and by cross calibration to the yield obtained with a 0.5 mm Au capture sample. Self-shielding, multiple scattering and γ-attenuation have been evaluated and found to be small for our thin samples.
When background data obtained with ^{208}Pb are used, our results for ^{105}Pd deviate from those of ORNL systematically by approximately + 10 % below 10 keV neutron energy whereas at higher energies the data are in agreement within $\pm$ 5 % except for the last energy bin. The average capture cross sections show a systematic decrease with the atomic weight for the even isotopes. For these isotopes, our results compared to those of ORNL show systematic deviations similar to that of ^{105}Pd, namely:

^{104}Pd : approximately + 10 % below 15 keV and at higher energies agreement within $\pm$ 6 %

^{106}Pd : deviation of + 20 % below 15 keV and approximately + 7 % up to 150 keV

^{108}Pd : deviation of 10 % below 15 keV, reducing to 20 % for higher energies

^{110}Pd : approximately 30 % deviation over the whole energy range considered.

---

* Rijksuniversitair Centrum, Antwerpen, Belgium

No explanation for the observed discrepancies could be found on the base of our experimental investigations. However, with the use of the black resonance technique the Geel data approach the values of ORNL.
A paper with the complete results analysed up to 300 keV has been presented at the International Conference on Nuclear Data for Science and Technology (Antwerp, September 1982).

1.4 GAS PRODUCING REACTIONS

Determination of $^{7}Li(n,n't)^{4}He$ cross sections

H. Liskien, R. Wölfle*, S. Qaim*

This work has been finalized and presented at the recent International Conference on Nuclear Data for Science and Technology (Antwerp, September 1982). The abstract reads as follows:

" Cross sections for the tritium-breeding reaction $^{7}Li(n,n't)^{4}He$ have been determined in view of their importance for the breeding factor of future fusion reactors and due to existing discrepancies. More than thirty samples have been irradiated with quasi-monoenergetic neutrons in the energy range from threshold to 8 MeV [D(d,n)] and from 13 to 16 MeV [T(d,n)]. Samples consisted of about 0.7 g metallic lithium enriched in ^{7}Li. The neutron fluences (10^{10} to 10^{11} cm^{-2}) have been determined relative to the 180° differential n-p scattering cross sections. The irradiated samples were transferred to a vacuum system and converted at 600-700°C by carrier hydrogen to lithium hydride (LiT). Thereafter, the temperature was raised to 800°C, the hydrogen carrier pumped off and aliquots collected in a 0.5 l proportional counting tube which was then filled up with methane and connected to a low background anticoincidence counting system. The measured cross sections have uncertainties of 6 to 7 %. They are higher than recent Harwell results but are consistent with the results of ANL at 7 and 8 MeV."

Our final results are summarized in Table 1.7 and Fig. 1.10.

Measurements of (n,α) cross-sections for Cr, Fe and Ni at 14 MeV neutron energy

E. Wattecamps, H. Liskien, F. Arnotte

Measurements have been made for elemental Cr, Fe and Ni using T(d,n) neutrons of 14 MeV produced with the CN Van de Graaff accelerator. Our results were presented under the above title at the International Conference on Nuclear Data for Science and Technology (Antwerp, September 1982). The abstract of

---

* Institut für Chemie der Kernforschungsanlage Jülich GmbH

Table 1.7 Final results of this work

E (MeV)	ΔE (MeV)	σ (mb)	Δσ (mb)
4.99	+ 0.23	95	+ 6
5.23	∓ 0.24	137	∓ 10
5.39	∓ 0.18	200	∓ 12
5.49	∓ 0.18	269	∓ 16
5.61	∓ 0.17	297	∓ 20
5.74	∓ 0.16	316	∓ 18
5.74	∓ 0.16	399	∓ 23
5.99	∓ 0.16	352	∓ 21
6.23	∓ 0.15	369	∓ 23
6.49	∓ 0.18	361	∓ 21
6.73	∓ 0.14	359	∓ 22
6.98	∓ 0.14	367	∓ 24
7.23	∓ 0.13	369	∓ 24
7.23	∓ 0.13	388	∓ 25
7.48	∓ 0.13	364	∓ 24
7.48	∓ 0.13	352	∓ 23
7.73	∓ 0.13	351	∓ 25
13.01	+ 0.12	322	+ 20
13.51	∓ 0.17	292	∓ 19
13.77	∓ 0.20	306	∓ 19
14.02	∓ 0.24	271	∓ 17
14.77	∓ 0.28	263	∓ 17
15.03	∓ 0.31	256	∓ 16
15.27	∓ 0.32	269	∓ 17
15.78	∓ 0.31	246	∓ 16
16.03	∓ 0.33	253	∓ 16

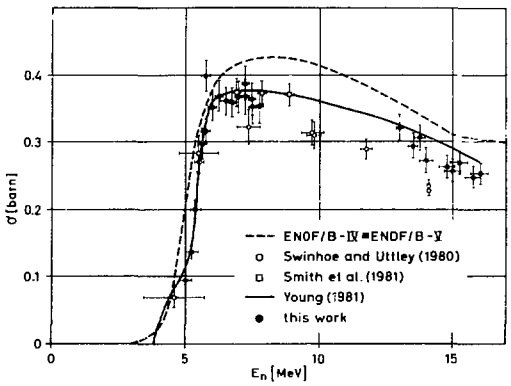

Fig. 1.10 Results of this work and other recent activation data compared with ENDF/B and a recent LANL evaluation

our contribution reads as follows:

" Helium production cross-sections for the main constituents of stainless steel (Cr, Fe, Ni) have recently been published for neutron energies between 5 and 10 MeV. The α-particles were detected with a multi-angle telescope and cross-section data relative to the well known n-p scattering cross-section were deduced. Those measurements have been performed now also at 14 MeV. At this energy the background condition had to be improved by changing the neutron collimation, by reducing the sensitive volume of the ΔE-proportional counters, and by replacing remaining low-Z material inside the chamber by tantalum. Listing mode data acquisition is used and α-particle identification is performed by transforming the observed (ΔE,E) signal into a (MZ^2,E) signal. The measurements yield the angle-differential cross-sections for five fixed angles. Angle-integrated cross-sections are compared with the few results available in literature."

The spectrum-average cross section ratio of $^{63}Cu(n,\alpha)^{60}Co$-to-$^{27}Al(n,\alpha)^{24}Na$ in a thick-target $^{9}Be(d,n)^{10}B$ neutron spectrum

H. Liskien, D.L. Smith*, R. Widera

This work has been presented under the above title at the recent International Conference on Nuclear Data for Science and Technology (Antwerp, September 1982). The abstract of our contribution reads as follows:

" A Cu-Al alloy sample has been irradiated in a potential 'benchmark' neutron field which was produced by bombarding a thick Be-target with 7 MeV deuterons. Due to the use of an alloy, and the close proximity of the involved γ-energies (^{24}Na: 1368 keV; ^{60}Co: 1333 keV), a very accurate value of 0.539 ± 0.009 was obtained for the spectrum average cross section ratio of $^{63}Cu(n,\alpha)^{60}Co$-to-$^{27}Al(n,\alpha)^{24}Na$. This experimental value is compared with calculated values as derived from differential cross section evaluations and spectrum information, and it is found to support the recent $^{63}Cu(n,\alpha)^{60}Co$ evaluation of Winkler et al.[1]".

1.5 VARIOUS MEASUREMENTS AND DEVELOPMENTS

Thick-target $^{9}Be(d,n)^{10}B$ neutron spectrum at E_d = 7.0 MeV

A. Crametz, H.-H. Knitter, D.L. Smith*, H. Bax, R. Vogt

A paper was presented at the International Conference on Nuclear Data for Science and Technology (Antwerp, September 1982), which describes the studies of the possibilities for cross section measurements in the 1 to 11 MeV range using the thick target $^{9}Be(d,n)$ source at E_d = 7 MeV; especially its potentiality in view of the expected availability of the post bunching system of the CN-Van de Graaff with its expected improved timing resolution of 250 ps. The abstract is as follows:

" The CBNM Van de Graaff will be equipped with a post buncher to reduce the pulse width from 1.5 ns down to about 250 ps. Therefore the $^{9}Be(d,n)^{10}B$ thick-target yield obtained by a pulsed 7 MeV deuteron beam was studied, especially in view of using this source for neutron cross section measurements in the energy range up to 11.3 MeV. For this purpose the spectrum shape was measured in this neutron energy range and the integral was normalized to values from literature. An absolute neutron fluence comparison was made between this source and the GELINA spectrum normalized to the same inverse velocity resolution of 0.1 ns.m^{-1}. In order to show the great potential of this source, the total cross sections of carbon

---

(1) G. Winkler, D.L. Smith, J.W. Meadows, Proc. International Conference on Nuclear Cross Sections for Technology, Knoxville, 1979, NBS Special Publication 594, page 199

* Visiting Scientist from ANL (USA)

and silicon were determined in an energy range from a few 100 keV to 11 MeV in a measuring time of a few hours with a statistical accuracy, e.g. at 6 MeV, of less than 2 %, and with an energy resolution of 60 keV. Comparison of the experimental results was made with the evaluated data sets of ENDF/B-V."

Neutron energy spectra from (α,n)-reactions in light elements

G.J.H. Jacobs*, H. Liskien

This work has been finalized. A manuscript with the title "Energy Spectra of Neutrons produced by α-particles in Thick Targets of Light Elements" has been prepared and will be submitted to Annals of Nuclear Energy.
The abstract reads as follows:

" Energy spectra of neutrons produced by 4 to 5.5 MeV α-particles in thick targets of C, Mg, Al, Si, BN, CaF_2, Al_2O_3, SiO_2, and UO_2 have been determined. A Van de Graaff accelerator has been used as pulsed α-particle source and neutrons were detected at 0°, 30°, 60°, 100°, and 140° by a calibrated NE 213 scintillator used as time-of-flight spectrometer. Angle-integrated spectra were derived not only for the above materials but also for B, F, and O. Energy integration delivers yields in good agreement with recent results from 4π moderator tank measurements."

Precise measurement of cross sections for the reactions $^{90}Zr(n,2n)^{89}Zr$ and $^{58}Ni(n,2n)^{57}Ni$ from threshold to 20 MeV

G. Winkler**, A. Pavlik**, H. Vonach**, A. Paulsen, H. Liskien

The work was presented, under the above title, at the recent International Conference on Nuclear Data for Science and Technology (Antwerp, September 1982).
The abstract reads as follows:

" The excitation functions for the reactions $^{90}Zr(n,2n)^{89}Zr$ and $^{58}Ni(n,2n)^{57}Ni$ were measured from 12.3 to 19.6 MeV in steps of 0.2-0.8 MeV using activation techniques. The reaction $T(d,n)^4He$ was used to produce the neutrons. Neutron fluences were determined by means of a proton-recoil telescope at 0° and the differential neutron production cross sections. Additionally, in the energy range 13.4-14.8 MeV measurements were performed in smaller energy steps (0.02-0.15 MeV) relative to well known cross sections for the reference reaction $^{27}Al(n,\alpha)^{24}Na$. Activity measurements were performed using a 12.7 cm x 12.7 cm NaI(Tl) well-type detector. The new cross section data were evaluated together with other experimental data from the literature to produce an improved set of evaluated group cross sections and their

---

* Bursary from TH Eindhoven; now with Océ Research Laboratory, Venlo

** Institut für Radiumforschung und Kernphysik der Universität Wien und der Österr. Akademie der Wissenschaften, Boltzmanngasse 3, A-1090 Wien, Austria

uncertainties for the reactions $^{90}Zr(n,2n)^{89}Zr$ and $^{58}Ni(n,2n)^{57}Ni$, including covariance information. Spectrum-averaged cross sections for the ^{252}Cf spontaneous-fission neutron field and the ^{235}U fission spectrum were calculated on this basis and compared with available experimental integral data."

Development of a detector for (n,charged particle) measurements

C. Bürkholz, J.A. Wartena, H. Weigmann

Development work on a detector for (n,charged particle) measurements at the linac has been started. It aims at a detector with the following features:

- Fast timing for high resolution time-of-flight measurements
- Identification of different charged particles (α,d,p) emitted
- Coarse information on the angular distribution of emitted charged particles
- Large solid angle for detection
- Allowance for large area samples to be used.

A first prototype, consisting of a 1 mm thick NE 102A plastic scintillator as E-detector and either an ionization chamber or a multiwire proportional counter as a ΔE detector, has been tested at a 13 m flight path station of the linac. With appropriate collimation and sufficiently thin sample backings, spectral distortions as a function of time of flight due to the linac γ-flash could be reduced to an acceptable limit (< 5 %).
The extraction of information pertaining to the angular distribution of emitted charged particles from the multiwire proportional counter is now under investigation.

Tests with C_6D_6 detectors

A. Brusegan, F. Corvi, G. Rohr, R. Shelley, T. van der Veen

The starting point of studies in connection with the weighting method, using C_6D_6 scintillators, was the use of the ^{56}Fe (1.15 keV) resonance for normalization. The application of this resonance for structural materials should have the following advantages:

1) the 1.15 keV resonance is an almost pure capture resonance ($\Gamma_n \ll \Gamma_\gamma$), hence the capture area can be determined very precisely in a transmission experiment
2) the γ-ray spectrum of this resonance is very hard, similar to those which have to be measured

3) the ^{56}Fe-isotope is present as an impurity in all iron samples, eliminating the need for a special normalization run
4) no extrapolation of the neutron flux from eV to keV range is needed, as would be the case for the Au and Ag resonances generally used for normalization.

With these conditions the accuracy of the capture data for iron isotopes depends mainly on the precision of the relative flux measurement.
The problem came to light because of the widely differing results of the capture area for the ^{56}Fe (1.15 keV) resonance obtained in the transmission experiment (Γ_n = 58 meV, Γ_γ = 610 meV, A_γ = 53 meV) and the capture measurement normalized to the low energy Ag-resonances (A_γ = 70 meV).
Very recently the capture area of the ^{56}Fe (1.15 keV) resonance normalized to Ag has been tested at Geel using different weighting functions (WF), the WFs plotted in Fig. 1.11.
The 'Old' WF is calculated with a Monte Carlo based computer code developed at Cadarache and Karlsruhe [1]. The same WF was obtained at AERE [2] using the routine GAMOC and a Fortran programme based on an analytical method developed at ORNL [3].
All three codes use a mathematical expression to calculate the most probable energy loss of the electrons in the scintillator.
The 'NEW' WF has been calculated using an increased energy loss of electrons in the scintillator employing newly evaluated data from Atomic Data [4].

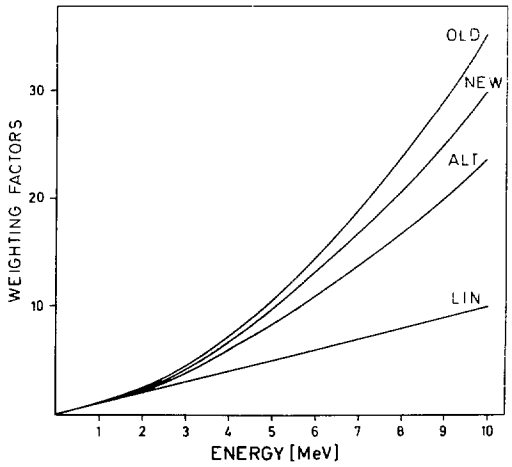

Fig. 1.11 C_6D_6 capture detector weighting functions

(1) C. Le Rigoleur, A. Arnaud, Proc. NEACRP/NEANDC Specialist Meeting on Neutron Capture in the keV Energy Range in Structural Materials for Fast Reactors, Karlsruhe, May 1973, Report KFK 2046 (1975)
(2) R.B. Thom, U.K. Nuclear Data Progress Report (Jan.-Dec. 1979), NEANDC(E)212 Vol. 8, p. 22
(3) R.L. Macklin, J.H. Gibbons, Phys. Rev. 159 (1967) 1009
(4) L. Pages et al., Atomic Data 4 (1972) 1

The 'ALT' WF includes γ-absorption in the sample and the scintillator containers by assuming an absorption of 40 % for a γ-ray energy of 330 keV, corresponding to the absorption in 1 mm of Ag (R = 4 cm) or in the Fe oxide samples used for the measurements at CBNM. As an upper limit the linear WF (LIN) has been added for comparison.

In Table 1.8 the capture areas normalized to Ag obtained for the different WFs have been listed for ^{56}Fe (1.15 keV) and, in addition, ^{57}Fe (1.6 keV) a newly measured pure capture resonance with the following resonance parameters obtained in a transmission measurement: Γ_n = (42.6 $\pm$ 0.4) meV and Γ_γ = (996. $\pm$ 300) meV (ℓ = 1, J = 2, g = 1.25). The transmission results for the pure capture resonances are given under TRA in the table.

Table 1.8 Test of weighting functions for ^{56}Fe (1.15 keV) and ^{57}Fe (1.6 keV) resonances

Weighting Function	^{57}Fe (1.6 keV) $g\Gamma_n\Gamma_\gamma/\Gamma$ (meV)	^{56}Fe (1.15 keV) $g\Gamma_n\Gamma_\gamma/\Gamma$ (meV)
O L D	54.	70.
N E W	51.5	65.
A L T	49.	61.
L I N	41.	49.
T R A	51.	53.
$< w >$	20.5	28.9

In the case of ^{57}Fe excellent agreement is obtained between the transmission value and the capture result using the 'NEW' weighting function. On the other hand to get a similar agreement for ^{56}Fe it becomes necessary to utilize a WF that is nearer to the 'LIN' one. There is no WF for which transmission results for both ^{56}Fe and ^{57}Fe can be reproduced. However, we conclude that the weighting method can be used confidently at least for resonances with an average weight up to $< w >$ = 20.5. The method fails for the ^{56}Fe (1.15 keV) resonance with $< w >$ = 28.9, where the capture area is overestimated by 22.6 % using the NEW weighting function.

In order to determine the upper limit of the validity of the pulse height weighting technique and to study the behaviour of the detector beyond this limit, more pure capture resonances with different $< w >$ have to be measured.

But there is a possibility of getting this information by comparing results from other capture detectors which do not depend so strongly on the spectral shape [1].

Shielding power of B-loaded resin/cadmium sandwiches

C. Bastian, H. Riemenschneider

As a first application of the Monte Carlo workspace COLLGEEL, a close-to-life simulation of a neutron shielding wall was performed. The geometry (see Fig. 1.12) bases on thicknesses actually used around Linac experiments.

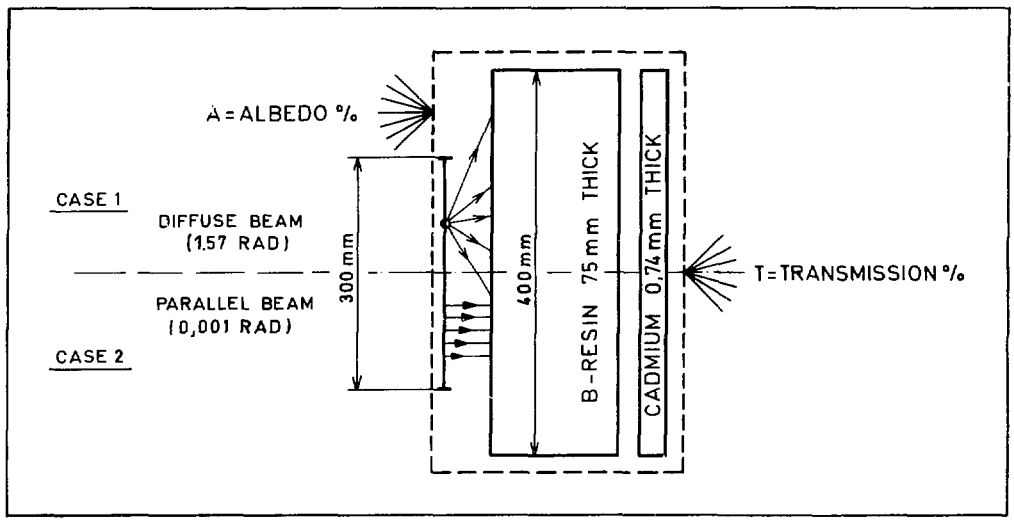

Fig. 1.12 Shield simulation geometry

The material composition of the borax-loaded epoxy resin was determined by chemical analysis (courtesy Mr. Le Duigou, CBNM, et al.). The results in percent of weight were as follows: C: 33.5 ± .3; H: 4.45 ± .5; B: 4.5 ± .2; Na: 8.25 ± .15; O: 49.3 ± .25. Atomic concentrations deduced from these results were stored in the workspace together with group cross section data from the VITAMIN C library (177 groups, origin: ENDF).
Two cases were simulated: a "hard" parallel beam hitting the wall normally and a "diffuse" beam with neutrons coming from any direction in the non-shielded halfspace.

(1) G. Rohr, Proc. of the Specialists Meeting on Fast-Neutron Capture Cross Sections (Argonne, April 1982) to be published

The initial energy of the neutrons covered the range 1 eV - 1 MeV in 12 monoenergetic values. The results of 300 - 500 simulated histories per energy value are summarized each as a transmission and an albedo value in % (see Fig. 1.13).

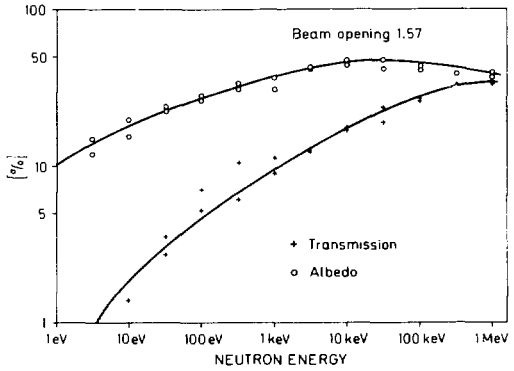

Fig. 1.13 Neutron shielding with boron loaded resin

We found out that nearly all absorptions occurred in the resin and not in the cadmium. This is certainly due to the high moderation and absorption power of the boron loaded resin. In this simulation all neutrons moderated below .1 eV were counted as absorbed. The present results should therefore not be extrapolated down to the thermal neutron beams, for which an ad hoc simulation could be performed if required.

1.6 STANDARD NEUTRON DATA

$^6Li(n,t)^4He$ standard cross section

H.-H. Knitter, C. Budtz-Jørgensen, D.L. Smith*, H. Bax, R. Vogt

A paper "Determination of the $^6Li(n,t)^4He$ Standard Cross Section" was prepared for and presented at the Internationl Conference on Nuclear Data for Science and Technology (Antwerp, September 1982). The abstract reads as follows:

" The neutron total and differential neutron elastic scattering cross sections of ^6Li were measured at the Van de Graaff with monoenergetic neutron beam and time-of-flight techniques in the neutron energy range from 80 keV to 3.0 MeV, yielding the angle integrated $^6Li(n,t)^4He$ cross section from 80 keV to 500 keV with an accuracy ranging from 2.5 % to 6.5 %. Angular distributions of the tritons with respect to the incident neutron beam direction were measured with the pulsed white spectrum neutron source GELINA in the neutron energy range from 10 eV to 330 keV. Both experiments were combined to give the absolute differential $^6Li(n,t)^4He$ cross section in the debated region of the resonance. A comparison of recent cross section shape measurements in the resonance region, which were normalized at low neutron energies to the $^6Li(n,t)^4He$ cross section itself, show good agreement with the present cross section measurements for which the absolute scale does not depend from other

---

* Visiting Scientist from ANL (USA)

experiments. A further comparison of the present differential (n,t) cross section for zero and 180 degrees shows excellent agreement with the same quantity determined by Brown et al. from the measurement of the zero degree laboratory ^{6}Li yield of the inverse reaction ^{3}H(^{4}He,^{6}Li)n, which was normalized relative to the ^{3}H-^{4}He elastic scattering cross sections."

Low energy particle detection with the Xe scintillator

C. Bastian, H. Riemenschneider

The scintillation pulses produced in Xenon by the ^{10}B(n,α) reaction products could not be separated completely from low level pulses also seen with ^{6}Li and ^{235}U samples. Accordingly a series of measurements were performed with a ^{10}B, ^{6}Li and a dummy sample consisting of a bare aluminium coating at the inside of the cylindrical support.

The pulse height spectrum obtained with the dummy sample coincides with the low level component of the one obtained with the ^{6}Li or the ^{10}B sample (see Fig. 1.14). This may be partly explained by neutron induced nuclear reactions in Xenon, as apparent from the 9 and 11 eV Xe resonances in the recording of the data obtained with the dummy samples. Besides a continuum counting level is attributed to a reproducible noise component at low amplitude. It is therefore possible to separate the ^{10}B(n,α) products without undue amplitude discrimination, by simply deducing the recording of the dummy sample under the same irradiation.

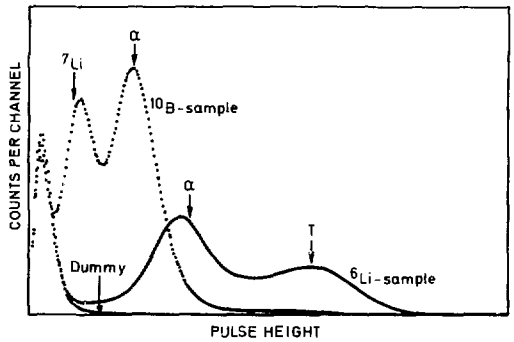

Fig. 1.14 Xenon-scintillator pulse height distribution

Determination of detection efficiencies of ionization chambers for standard cross section measurements

C. Budtz-Jørgensen, H.-H. Knitter, R. Arlt*, R. Vogt

The correction for losses of reaction products in the investigated sample is of importance for high precision cross section measurements. Calculations of such losses need the knowledge of angular distributions and have to be

---

* Visiting Scientist from TU Dresden (GDR)

based on assumption of the effective thickness of the employed sample and of the ranges of the emitted particles which are difficult to verify experimentally. In the present investigation a gridded ionization chamber was used in order to measure the sample losses directly. As it has been demonstrated [1] such a detector can give information about the direction of the reaction product. The signals obtained from the anode of the detector are proportional to the particle energy, whereas the signals from the cathode depend on both the energy and cosine of the angle θ between the particle direction and the normal to the sample. Applying a suitable processing of these signals a quantity proportional to cos θ can be derived. Fig. 1.15 shows the cos θ distribution for fission fragments stemming from a self-transferred ^{252}Cf source. The isotropy of the emitted fragments is reflected by the rectangular distribution. Fig. 1.16 shows the similar distribution for fission fragments produced in a 100 μg/cm^2 thick ^{235}U sample by thermal neutrons. This shape is also rectangular but a loss of events near cos θ = 0 is apparent. By comparison to the "infinitely" thin ^{252}Cf sample one can derive the loss of fragments in the ^{235}U sample.

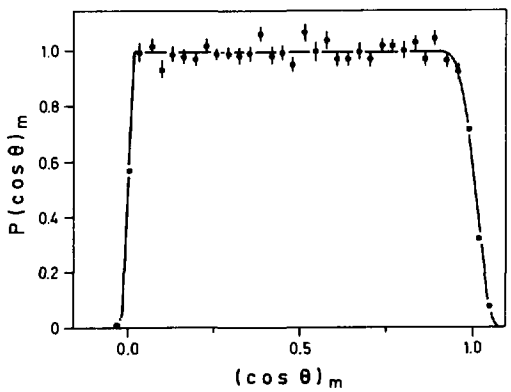

Fig. 1.15 Cos θ distribution of fission fragments from self-transferred ^{252}Cf source

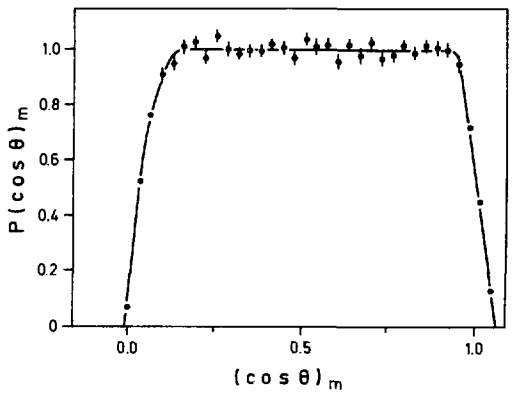

Fig. 1.16 Cos θ distribution of fission fragments from ^{235}U bombarded with thermal neutrons

A series of measurements where this efficiency of the fission detector is studied as function of sample type, sample thickness and neutron energy has been started.

---

(1) H.-H. Knitter, C. Budtz-Jørgensen, Proc. of the Intern. Conf. on Nuclear Cross Sections for Technology, Knoxville 1979, NBS Special Publication 594, page 947 (1980)

1.7 UNDERLYING PHYSICS

Neutron induced charged particle reactions on ^{23}Na

H. Weigmann, G.F. Auchampaugh*, P.W. Lisowski*, M.S. Moore*, G.L. Morgan*

This work has been finished and a contribution has been presented to the International Conference on Nuclear Data for Science and Technology (Antwerp, September 1982), with the following abstract:

" High resolution measurements of neutron induced charged particle reactions on ^{23}Na have been performed. A NaI(Tl) detector served as both target and detector, with pulse shape discrimination being applied for the separation of protons and alpha-particles from each other and from events involving gamma-ray detection. The neutron energy was measured by time-of-flight, using an 80 m flight path at the Los Alamos National Laboratory WNR facility. Relative cross sections for $^{23}Na(n,p)$ and $^{23}Na(n,\alpha)$ have been determined in the neutron energy range between 5 and 11 MeV. Up to 9 MeV it has also been possible to separate the (n,p) reaction leading to the ^{23}Ne ground state from the (n,p') reaction feeding the first five excited states of ^{23}Ne. All observed cross sections show strong fluctuations in most of the energy intervals investigated, especially below 7 MeV, where marked peaks are observed in the (n,p) cross section. In the range between 7 and 9 MeV neutron energy, a significant correlation is found between the fluctuations in the (n,p) and (n,p') cross sections, whereas the fluctuations in the (n,α) cross section are not correlated with either of the former two. This observation is indicative of doorway states common to the proton channels, possibly due to states in ^{24}Na with isospin $T = T_Z + 1$."

Neutron resonance parameters of ^{32}S

C.R. Jungmann**, E. Cornelis+, L. Mewissen++, F. Poortmans++, J.P. Theobald+++, H. Weigmann

This work has been finished and a paper published in Nuclear Physics A, with the following abstract:

" Neutron transmission experiments were performed on ^{32}S between 0.18 MeV and 19 MeV and differential elastic scattering experiments up to 2 MeV. The resonance parameters, including spin and parity, were determined up to 1.7 MeV. The distribution of neutron strength was determined for $s_{1/2}$, $p_{1/2}$, $p_{3/2}$, $d_{3/2}$, $d_{5/2}$ and f-wave levels, and is compared to recent model calculations. The isotopic purity of some possible T = 1/2 isobaric analogue states was deduced from their neutron widths."

---

* Los Alamos National Laboratory, Los Alamos, N.M., USA

** Bursary of the European Community

+ Rijksuniversitair Centrum, Antwerpen, Belgium

++ SCK/CEN Mol, Belgium

+++ Institut für Kernphysics, T.H. Darmstadt

The $^{33}S(n,\alpha)^{30}Si$ reaction in the resonance region

C. Wagemans*, H. Weigmann, R. Barthélémy

A higher resolution experiment was performed at a 30 m flight-path. A partial result is shown in Fig. 1.17, which gives the $^{33}S(n,\alpha)$ cross-section in the neutron energy region from 10 keV up to 1 MeV. These data will be further analysed and interpreted.

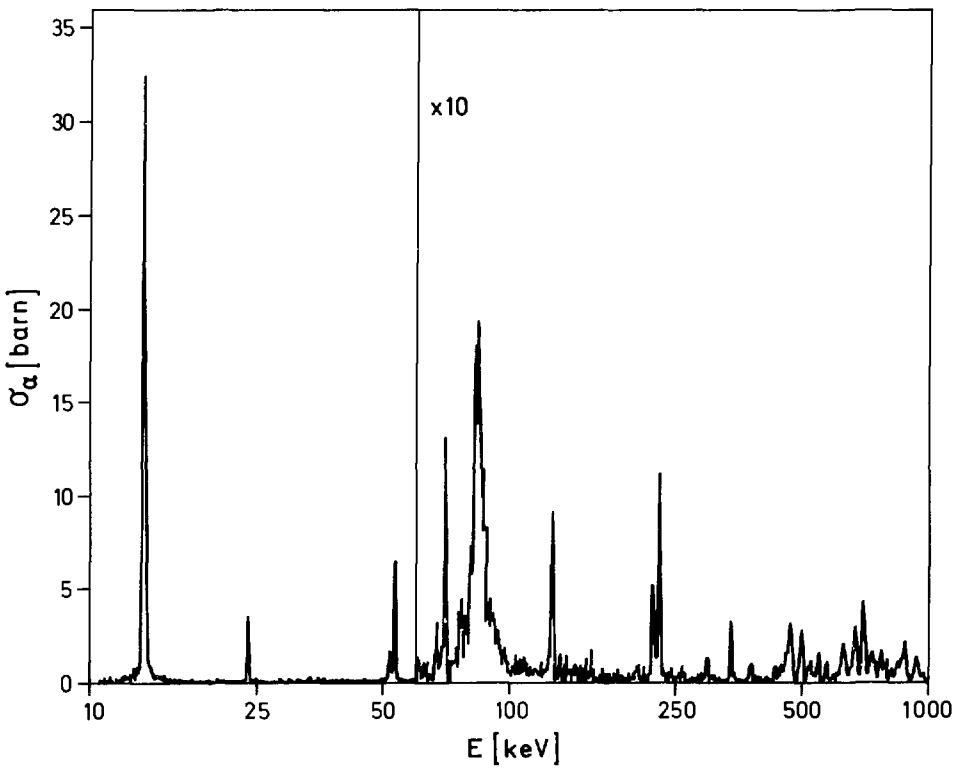

Fig. 1.17 The $^{33}S(n,\alpha)^{30}Si$ reaction cross-section in the neutron energy region from 10 keV to 1 MeV

Fission fragment angular distributions and kinetic energies for $^{235}U(n,f)$ and $^{232}Th(n,f)$

J. Meadows**, C. Budtz-Jørgensen, H. Bax

A contribution, "Fission Fragment Angular Distributions and Total Kinetic Energies for $^{235}U(n,f)$" has been presented to the International Conference

* SCK/CEN Mol and R.U. Gent, Belgium

** Argonne National Laboratory (USA)

on Nuclear Data for Science and Technology (Antwerp, September 1982). The abstract of the paper is:

" A gridded ion chamber was used to measure the fission fragment angular distribution and total kinetic energy for the $^{235}U(n,f)$ reaction from 0.18 to 8.81 MeV neutron energy. The anisotropies are in generally good agreement with earlier measurements. The average total kinetic energy is ~ 0.2 MeV greater than the thermal value at neutron energies < 2 MeV and shows a sudden decrease of ~ 0.8 MeV between 4 and 5 MeV neutron energy, well below the (n,n'f) threshold. The decrease near 5 MeV may be due to the change in the mass distribution."

A paper "Angular Distribution and Total Kinetic Energy for $^{232}Th(n,f)$" was presented at the Symposium on Nuclear Fission and Related Collective Phenomena, Bad Honnef 1981. The abstract of the paper is:

" A measurement of the $^{232}Th(n,f)$ fission fragment angular distributions with incident neutron energies from 1.5 to 1.8 MeV and energy spread of + 8 keV is described. A channel analysis based on the measured angular distribution is presented. The fragment total kinetic energies were measured simultaneously and a dramatic $\overline{TKE}$ variation of ≈ 1 MeV was observed over the $^{232}Th(n,f)$ resonance at 1.6 MeV."

Barrier heights of plutonium isotopes

H.-H. Knitter, C. Budtz-Jørgensen, H. Bax

The evaluations of the second chance fission thresholds of the plutonium isotopes with a simple physical model were completed and the results are contained in a paper "Barrier heights of plutonium isotopes from (n,n'f)-thresholds" presented to the International Conference on Nuclear Data for Science and Technology (Antwerp, September 1982). The abstract reads as follows:

" The neutron induced second chance fission cross section for the isotopes ^{238}Pu, ^{239}Pu, ^{240}Pu, ^{241}Pu, ^{242}Pu, and ^{244}Pu are studied in the region of the threshold using a simple model. Numerical values are obtained for the inner fission barrier heights of the mentioned isotopes and of the nuclear temperatures governing the neutron evaporation process at incident neutron energies around the second chance fission threshold. The comparisons of the present parameters with those obtained by other methods give hints to possible insufficiencies of experimental cross section data in the region of the second chance fission threshold."

Fission fragment mass distribution of ^{252}Cf

Ch. Straede*, C. Budtz-Jørgensen, H.-H. Knitter

Previously performed measurements on the spontaneously fissioning ^{252}Cf were evaluated with respect to their mass distribution, in order to test a method to measure fission fragments mass and angular distributions together in the same experiment by a double ionization chamber with Frisch grids where both fragments are detected.

In Fig. 1.18 the full dots show the pulse height spectrum generated by ^{252}Cf fission fragments in our ionization chamber. For comparison, the open circles show the corresponding pulse height spectrum measured by Schmitt et al.[1] with a Si-surface barrier detector.

The difference in shape of the two spectra is assumed to be due to the difference in ionization mass defect for methane and silicon.

The present provisional mass distribution, ignoring the ionization mass defect, is plotted in Fig. 1.19 with full squares. The full circles in Fig. 1.19 represent the provisional mass distribution where the correction for the ionization mass defect was performed according to the "Schmitt-procedure" using the numerical data for Si-surface barrier detectors.

As shown in Fig. 1.19, this is an important correction and has later to be done with better numerical values determined specifically for our counter gas.

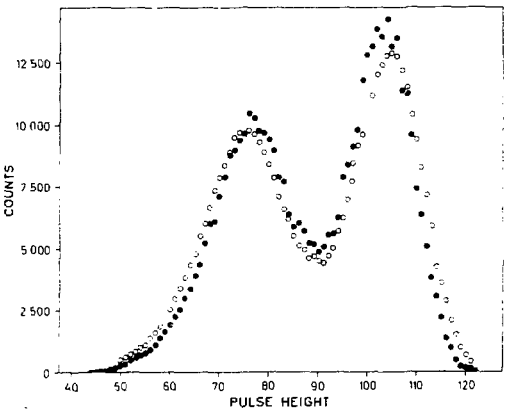

Fig. 1.18 Fission pulse height spectra of ^{252}Cf

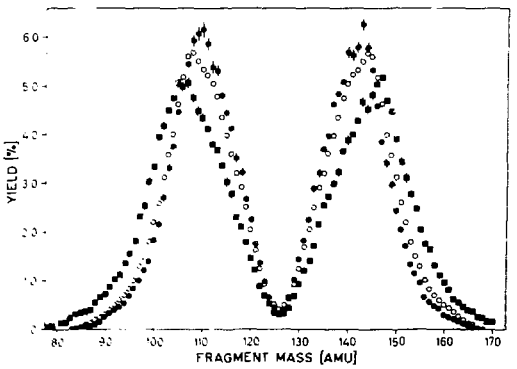

Fig. 1.19 Provisional fission fragment mass distribution of ^{252}Cf

(1) H.W. Schmitt, W.E. Kiko, C.W. Williams, Phys. Rev. B137, 837 (1965)

* Bursary from University Aarhus

Comparison is made in Fig. 1.19 with the corresponding provisional mass distribution of Schmitt et al., open circles, which was measured with Si-surface barrier detectors.

1.8 MAJOR RESEARCH EQUIPMENT

Electron linear accelerator

J.M. Salomé, R. Cools, R. Forni, F. Massardier, F. Menu, K. Meynants, P. Siméone, F. Van Reeth, J. Waelbers, C. Waller

During the covered period (01.11.1981 to 1.10.1982), the accelerator was operated as shown in Table 1.9. On the average, 5.2 neutron beams were used simultaneously for neutron measurements. Low energy electron beams, with mean currents of 40 to 65 μA at 36 and 44 MeV were produced six times for activation analysis.

Table 1.9 Operational parameters of the linear accelerator

Pulse lenght ns	Rep. rate Hz	Peak current A	Mean energy MeV	time h	time %
4 - 5	800	12	110	2211	70
10 - 18	40 - 100	11 - 7	100	588	19
2000	25 - 100	0.20	90	220	7
1600	300	0.14	36 - 44	110	3
Miscellaneous				24	1

Modifications at the injection side were achieved at the end of last year. They concern the magnetic field between the cathode and the input of the first section as well as the installation of a new prebunching cavity. The Linac operation was interrupted in August to allow for decay of the radioactivity in the target room before installing the pulse compressing magnet. Most of the radioactive parts used in this room were removed to

a storage room. The magnet has arrived at CBNM in October, entered and placed in the right position. The installation of the vacuum chamber, coils, pumps, water cooling system was finished at the end of this month. Several parts of the accelerator have been renewed or repared such as focusing quadrupoles, steering coils, windows, vacuum pumps. Beginning November, a vacuum of 10^{-8} torr in the accelerator and up to 3.10^{-6} torr in the magnet chamber were achieved. Measurements of the trajectories in the magnet with long pulses and narrow electron energy spectra were realized at the end of November to check the performance of the magnet. They will be followed by investigations of the pulse compressio features of the magnet.

Van de Graaff accelerators

Operation and maintenance
A. Crametz, P. Falque, J. Leonard, W. Schubert

During the 244 working days in 1982 - which corresponds to 1952 normal working hours - the total available machine time was 3106 hours. The break-down of this number is given below:

	CN - 7 MV		KN- 3.7 MV	
Accelerator running		1522		654
experiments	1339		633	
adjustments	84		21	
conditioning	99*		---	
Maintenance		200		---
Stopping hours for outside firms		271		
Pulse compression - Automation		459		

* not manned

- The tank of the CN has been opened 9 times: 6 times for maintenance including 3 exchanges of ion source, one was leaking under gas pressure, 3 times for improvements. Due to mechanical vibrations, the 1.5 kW alternator mounted on top of the column had to be replaced by another one which however delivered only 90 V instead of 110 V. After repair of the axis and replacement of bearings, the original alternator has been reinstalled.

- In April a complete new system for the storage of targets and their exchange on the 3 beam tube extensions has been installed.
- In September, October, accelerators were stopped because of the installation of ducts for the ventilation below the target hall by an outside firm and some experiments were performed during night hours.
- Neutron and gamma doses in the target hall.
  The neutron and gamma doses in the target hall have been determined for four typical accelerator conditions. Both conditions summarized in Table 1.10 were used with a target current of 15 and 5 μA - DC.

Table 1.10 Data used for the measurements

Nuclear reaction chosen	Neutron energy in MeV	Neutron angle degrees	Target material	Target thickness mg/cm²	Average ion beam energy-keV	Energy loss in half the target-keV	Ion beam energy in keV	Frequence of NMR in MHz
T(d,n)	23.000 20.840 16.392	0 45 90	TiT	2.0	5962.7	72.3	6035	46.191
D(d,n)	9.000 7.100 3.891	0 45 90	TiD	0.20	5790.6	7.5	5798	45.272

An example of the spatial distribution of the neutron dose is represented in Fig. 1.20. Besides interest for health physics consideration, it has been shown that the disturbance of an experiment at the 3.7 MeV accelerator by a neutron experiment conducted at the 7 MV accelerator, is not determined by direct target neutrons, but by room-scattered neutrons.

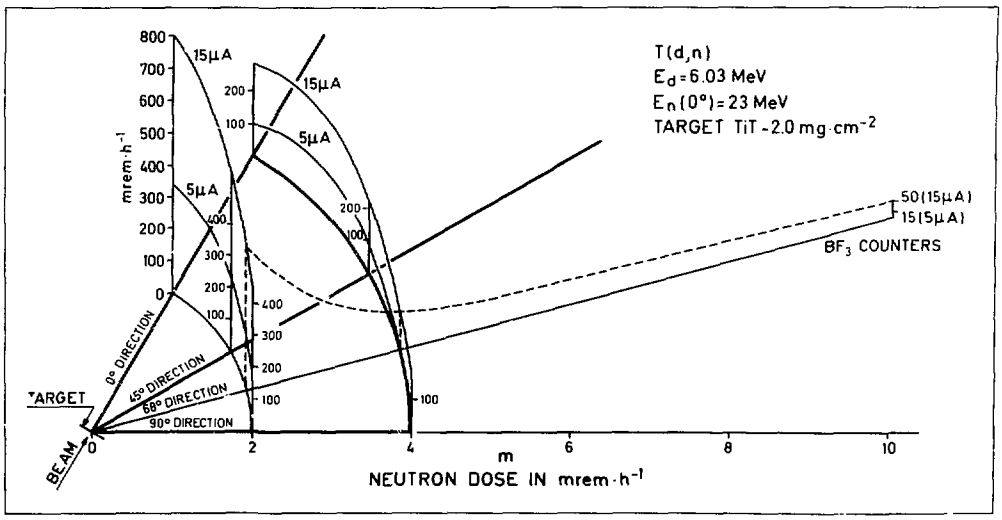

Fig. 1.20 Neutron dose in mrem·h^{-1}

Pulse compression with a spiral resonator
A. Crametz, S. de Jonge, F. Falque, J. Leonard, W. Schubert

To reduce the pulse width of presently 1.5 ns of the CN-7 MV accelerator by a factor 6 or more, a post bunching system has been installed between the analyzing and switching magnet (see Fig. 1.21).

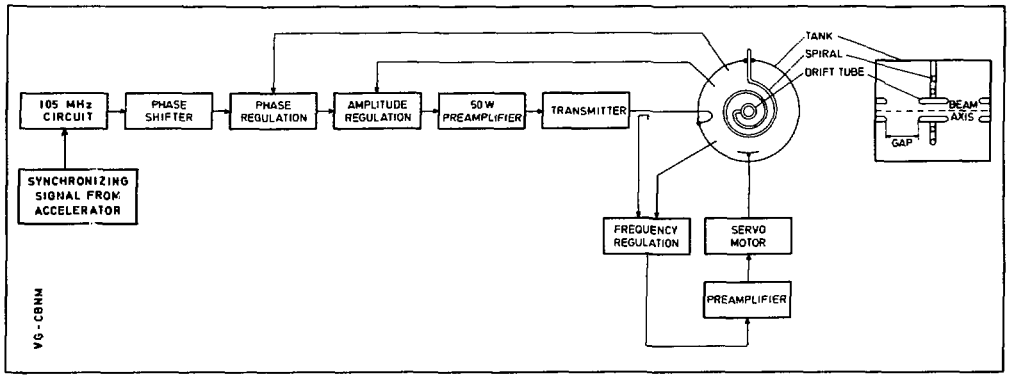

Fig. 1.21 Block diagram of a spiral resonator. The length of the gaps and of the drift tube are 2.0 and 9.4 cm, respectively

It consists of an Archimedian spiral in the cross section plane of a circular tube. The axis of the drift tube at the free end of the spiral is the flight direction of the particle. The length of the drift tube is calculated for a relative design velocity $\beta_o = \frac{V_o}{C} = 0.08$. The spiral is grounded by a "leg" on the tank (a cylinder of $\emptyset$ = 40 cm and ℓ = 23 cm). The resonator is closed by two metallic endplates parallel to the spiral plane. The RF power is inductively coupled by a tunable loop near the leg of the spiral and the thermal frequency shifts are compensated by a servo-operated tuning plate. Under resonance conditions peak voltages up to 150 kV are obtainable.
The 20 kW - 105 MHz transmitter has been adjusted, the electronic controlled and a vacuum inside the resonator of better than 10^{-6} Torr obtained with a cryogenic pump. For a DC deuteron beam of 3 MeV, and using a detector chain from Heidelberg, a timing resolution of 330 ps has been obtained. A repetition of this test with own (and faster) detector chains awaits delivery of ordered relevant material. Work concerning the synchronization is going on. In a first attempt using a LED emitter in the HV terminal and a receiver at ground potential, both connected by an optical fiber, limitation was found

for the field gradient of the optical fiber. In a second test with RF emitter and receiver, it has been demonstrated that a 2.5 MHz signal, which is the basic pulse repetition rate of the accelerator, cannot be transmitted inside the tank, but a 105 MHz signal. This signal is obtained from the 2.5 MHz reference signal in the terminal when multiplied by a factor 42 in a phase-loop. This possibility is at present under realization.

Automation
T. Babeliowsky, A. Crametz, A. De Keyser, W. Schubert, C. Van Rillaer

In order to have the accelerator under computer control, mechanical and electrical modifications of the command selsyns and switches were started. As an example, Fig. 1.22 represents the modified belt charge system.

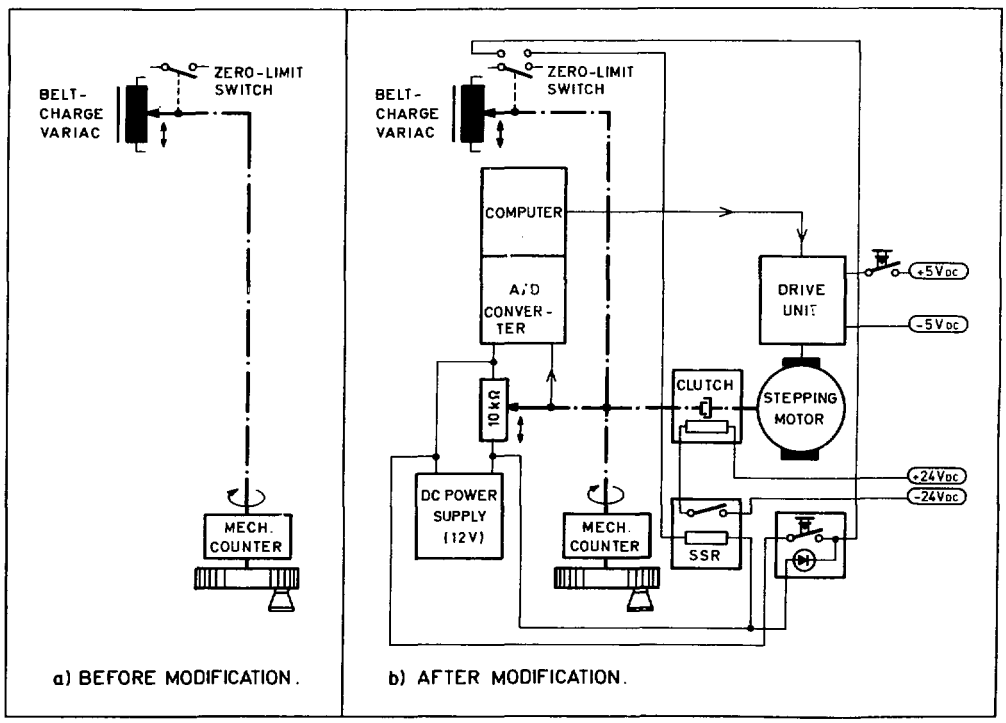

Fig. 1.22 Belt charge system

A programme has been written for an Apple II computer. We dispose now of a protocole listing, as shown in Table 1.19, where all the parameters of the accelerator are reported at regular time intervals. In order to attract the

attention of the operator and to indicate him where he should react, not only an acoustic alarm is given, but also an extra line is printed if one parameter is changing by more than 10 %. This extra line only contains the time and the parameter in question. The programme is also planned to stop the accelerator in an organized manner if the target current is outside pre-selected limits.

Computer aided design of neutron beam collimators

C. Bastian

The APL workspace COLLGEEL provides a Monte Carlo simulator of the neutron scattering and absorption in a set of rotation symmetric material rings. No intrinsic limit is put either on the number of rings, or on the complexity of their chemical composition, or on the energy dependence of their neutron cross sections.
Many neutron histories are simulated in parallel and the user follows their evolution step by step on a continuously updated, full screen status report. He may interrupt the simulation any time to modify the geometry or composition of the rings, the characteristics of the incoming neutron beam, etc ...

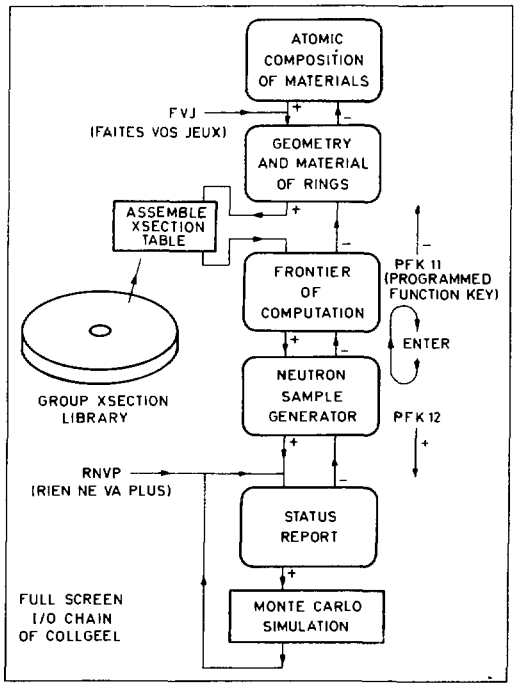

Fig. 1.23 Scheme of simulator

This is done in a chain of full screen accesses to the simulation parameters (Fig. 1.23).
During this process, the necessary cross section values are selected automatically from a 171 energy group library on disk.
This work will be presented as an example of Monte Carlo parallel simulation at the APL 82 Conference (July 26-30, Heidelberg).

Table 1.19 Protocole listing

DATE 15/12/82 FREQUENCY= 18908 KHZ EXTENSION USED= L3
GAS SELECTOR= H GAS= 28 TURNS SOURCE MAGNET= 24 TURNS
MODE=D.C.

TIME	VOLT	CL	VAC	COR	BEL	STEERER	FO	BE	EX	EL	30	STE	VERT-QUAD	ANA	ANAL-QUAD	SWI	EXT-QUAD	FR	PULSED MODE CH	PU	BU	BU	VAC	AMP	REBUNCHER TUN	INCI	REFL	TARG
	MEV	uA	TOR	uA	uA	X	Y	T	T	T	T	T	T	AMP	AMP	AMP	AMP	AMP	AMP	AMP	T	PH	AM	PH	AM		PLA	POWR	POWR	CURR
															MAG				MAG		SE	T	T	T	T	TOR	V		KW	KW	uA
16.17	2.05	5.	2.8		40.	13.	.54	10	15	24	1.	14		79.		46.													4.56
16.22	2.05	4.	3.0		42.	12.	1.3	10	15	24	1.	14		79.		46.													4.59
16.24	2.05	5.	2.8		40.	13.	.34	10	15	24	1.	14		79.		46.													4.01
16.26	2.05	4.	2.8		40.	13.	.84	10	15	24	1.	14		79.		46.													4.02
16.27							7.																						
16.28	2.05	4.	2.9		43.	12.	1.0	6.	15	24	1.	14		79.		46.													1.88
16.28																													1.75
16.29	2.05	4.	2.8		40.	13.	.24	6.	15	24	1.	14		79.		46.													1.57
16.31	2.05	4.	2.9		43.	11.	.74	10	15	24	1.	14		79.		46.													4.02
16.33	2.05	5.	2.8		40.	13.	.34	10	15	24	1.	14		79.		46.													4.47
16.35	2.05	4.	3.0		43.	12.	.94	10	15	24	1.	14		79.		46.													3.88
16.37																													1.38
16.37	2.05	5.	2.8		41.	12.	-.1	10	15	24	.9	14		79.		46.													.046
16.38	2.05	4.	2.8		40.	13.	.44	10	15	24	1.	14		79.		46.													.046
16.40	2.05	4.	2.8		40.	13.	.14	10	15	24	1.	14		79.		46.													.046
16.41	ACCELERATOR STOPPED																												

1.9 MISCELLANEOUS

Organization by CBNM of the "International Conference on Nuclear Data for Science and Technology, Antwerpen, 6-10 September 1982"

K.H. Böckhoff

The Antwerp Conference 1982 on Nuclear Data for Science and Technology continues a long sequence of application oriented nuclear data conferences. Their origin may be dated back to the sixties when the Washington/Knoxville series was launched in the USA with subsequent meetings in 1966, 1968, 1971, 1975 and 1979. IAEA contributed to the sequence with international conferences in 1966 (Paris) and 1970 (Helsinki). In the USSR meetings of similar scope were held within the Kiev series in 1971, 1973, 1975, 1977 and 1980. (Besides these data conferences there have been several nuclear physics oriented conferences, one of them also at Antwerp in 1965).
Based on the initiative of B. Rose and starting with the Harwell Conference in 1978, the previously largely uncorrelated series of nuclear data conferences was given a rigid scheme with respect to timing and location. It was agreed to hold annual meetings with the location cycled between Europe, the USA and the USSR. In the spirit of this agreement the Harwell Conference was followed in 1979 by the Knoxville Conference and in 1980 by the Kiev Conference. Once through with this cycle the turn was then again on Europe and upon request of the Nuclear Energy Agency Nuclear Data Committee, the Central Bureau for Nuclear Measurements accepted to organise the following Conference. There was at that time a broad concensus within the Western Nuclear Data and Reactor Physics Communities to enlarge the period between subsequent conferences of this type from one year to two years. The decision was then made to hold the Conference in 1982 in Antwerp and an agreement was achieved for a cooperation with NEANDC and IAEA and for sponsorships by the Belgian Nationaal Fonds voor Wetenschappelijk Onderzoek, the University of Antwerp, the European Physical Society, the International Union for Pure and Applied Physics and the City of Antwerp.
A Local and an International Programme Committee, the latter one extended by corresponding members, formed the advising body for the organization and the programme of the Conference.
The scope of the Conference was decided to be similar to that of its predecessors, emphazising Nuclear Data and Neutron Physics which pertain to fission and fusion energy programmes, but considering also nuclear data for

bio-medical purposes, astrophysics and solid state research. Underlying Physics, in particular the present picture of our understanding of neutron induced nuclear reactions completed this scope.
The Conference was attended by 270 scientists from 35 countries, among them for the first time also a delegation from the People's Republic of China.
A total of 229 contributions were presented, including 10 invited papers. The number of papers in this category has been drastically cut down, as compared to previous conferences.
For the first time in the history of such conferences, poster presentations were introduced. In fact, about 2/3 of all contributions were given as posters. Taking this option, rather than that one of parallel sessions, was not an easy decision. The organizers of the Conference were well aware of an intrinsic concern about poster contributions, dominant within the scientific community, which still considers posters as third class contributions. In the opinion of the organizers, however, poster presentations offer - if sufficient care is taken - an excellent chance for scientific communication, which may be better than that of the usually numerous, short oral presentations with their very limited discussion times. They address to a smaller audience of interested colleagues and discussion can be more profound and extended.
A number of measures have been taken to avoid discrimination of contributions with poster presentation against those with oral presentation.

- Both were considered as fully equivalent. Consequently texts of all these contributions entered into the Proceedings and were there reproduced without reference to their form of presentation at the Conference.
- All posters were on display during the whole period of the Conference.
- There have been five poster sessions of about one hour each, during which the stands of the indicated poster group had to be manned.
- The authors of contributed papers with poster presentation were invited to indicate themselves two periods of minimum one hour each during which their stand would be manned in addition to the period prescribed by the organizers of the Conference.
- The spatial sequence of poster pannels was interrupted by numerous white boards to ease discussions.
- Pigeon holes were provided for each participant to facilitate appointments on a personal base.

This specific form of the organization of a conference was an experiment, which - following the reactions after the conference - found a positive reception. The future conferences will show whether the psychologic barrier against poster presentations has become smaller.

2. Non-Neutron Nuclear Data

A. Deruytter

2.1 DECAY STUDIES

Decay of $^{93}Nb^{m}$

R. Vaninbroukx, W. Zehner

The measurements for the determination of the half life of $^{93}Nb^{m}$ have been continued using Si(Li) detectors. Four sources prepared from two different samples have been measured 28 times over a period of 5.3 years.
The mean value of the preliminary result is: $T_{1/2}$ = (16.2 ± 0.4)a. This value agrees well with the value of (16.11 ± 0.19)a measured by Lloret [1]. The quoted accuracy of our result corresponds to a 1σ confidence level and takes into account random (± 0.2a) and systematic (± 0.2a) uncertainties. Since we still have a small increasing trend in our results in function of the time of observation we will continue the measurements over at least one more year.
A paper on earlier work on a niobium dosimetry intercomparison where CBNM participated together with 6 other laboratories from EC countries was presented by H. Tourwé, SCK-CEN Mol, at the 4th ASTM-EURATOM Symposium on Reactor Dosimetry, Gaithersburg, March 22-26, 1982 [2].
At the same symposium, Alberts et al. presented a paper where the measurement of the KX-ray emission probability of $^{93}Nb^{m}$ is described [3]. The result of P_{KX} = 0.107 ± 0.003 is in disagreement with our value of 0.116 ± 0.004,

---

(1) R. Lloret, Complément à la mesure de la période de décroissance radioactive du $^{93}Nb^{m}$, Radiochem. Radioanal. Letters 50, 113 (1981)

(2) H. Tourwé, W.H. Taylor, D. Reher, R. Lloret, H.J. Nolthenius, P. Wille, R. Schweighofer, Niobium dosimetry intercomparison in EBR II and BR2, Proceedings of the Fourth ASTM-EURATOM Symposium on Reactor Dosimetry, Radiation Metrology Technique, Data Bases, and Standardization, National Bureau of Standards, Gaithersburg, Maryland, March 22-26, 1982, edited by F.B.K. Kam (Oak Ridge National Laboratory, Oak Ridge, 1982) NUREG/CP-0029, Vol. 1, CONF-820 321/V1, p. 401 - ORA 30395

(3) W.G. Alberts, R. Hollnagel, K. Knauf, M. Matzke, W. Pessara, "Measurements with the Niobium Neutron Fluence Detector at PTB", presented at the 4th ASTM-EURATOM Symposium on Reactor Dosimetry, Gaithersburg, March 22-26, 1982

determined about 3 years ago[1]. In a first attempt to solve this discrepancy a PTB-type $^{93}Nb^{m}$ source (389-80) was prepared and the disintegration and KX-ray emission rates were determined at PTB. Then the source was recalibrated at CBNM. By these measurements the discrepancy between the PTB and CBNM results was confirmed and seemed very likely to be due to the efficiency calibration of the detectors used at both laboratories. Therefore, two PTB-type reference sources, a ^{57}Co source (281-80) and a ^{88}Y source (30-81), were prepared and calibrated at PTB and then sent to CBNM for comparison.
The results of the activity determinations at PTB and CBNM on the reference sources are given in Table 2.1.

Table 2.1 Activity determinations

Nuclide	Source	PTB measurements		CBNM Reference date (t_2)	Decay correction t_1 to t_2		Activity in Bq on t_2	
		Reference date (t_1) 0.00 h	Activity (Bq)	0.00 h	$T_{1/2}$ used (days)	F_t	PTB result	CBNM result
^{57}Co	281-80	1.1.80	245140 ± 0.5% *	1.10.81	271.9 ± 0.1	0.19613 ± 0.1 %	48080 ± 0.6 % *	48240 ± 0.3 % *
^{88}Y	30-81	1.3.81	63766 ± 0.5% *	1.8.81	106.6 ± 0.2	0.36978 ± 0.2 %	23579 ± 0.7 % *	23586 ± 0.3 % *

* Quoted uncertainty corresponds to 1σ confidence level and takes into account random and systematic uncertainties.

From the good agreement between the PTB and CBNM results it is obvious that the discrepancy obtained for the $^{93}Nb^{m}$ sources can not be due to differences in the calibration of the reference sources, at least in so far as ^{57}Co and ^{88}Y are concerned. It is, therefore, more probable that the discrepancy is due to the utilization of different calibration nuclides and different decay data.
It should be mentioned that PTB additionally to ^{57}Co and ^{88}Y is using for the calibration of their detector in the energy region 13-26 keV: ^{85}Sr(Rb KX); ^{111}In(Cd K_{α}) and ^{241}Am(γ 26.35 keV). CBNM was using additionally to ^{57}Co: ^{241}Am(Np-LX rays and γ 26.35 keV), ^{103}Ru(Rh KX) and ^{109}Cd(Ag KX); ^{88}Y(Sr KX)

(1) R. Vaninbroukx, The Use of Liquid Scintillation Counting Techniques for Decay Parameter Studies of Radionuclides Decaying via Low Energy Isomeric Transitions, in Chin-Tsu Peng, D.L. Horrocks, E.L. Alphen (eds.), Liquid Scintillation Counting. Recent Applications and Developments, Vol. I (Academic Press, New York, 1980) p. 191

was only added in the frame of this investigation. For the measurements of the KX-ray emission rates three different calibrated detectors were used, two Si(Li) detectors and one HP-Ge detector. Typical detection efficiency (ϵ) curves for sources on Cr-coated glass discs are given in Fig. 2.1. For each of the three detectors the ratio of (ϵ PTB-type)/(ϵ glass disc) sources were found to be constant within $\pm$ 0.3 to 0.4 % over the energy range considered here. The efficiency ratios are also given in Fig. 2.1.

The detection efficiencies for the KX rays were re-estimated in the following way:

(1) Linear regression through the experimental points obtained with all radiations from the nuclides used in the calibration;

(2) linear regression through the experimental points obtained with the KX rays of ^{88}Y; ^{103}Ru and ^{109}Cd and with the 26 keV γ ray of ^{241}Am;

(3) by assuming that, after correction for small differences in the transmission through the Be window, the detection efficiencies for the Nb-KX rays are the same as these for the Sr-KX rays (^{88}Y decay).

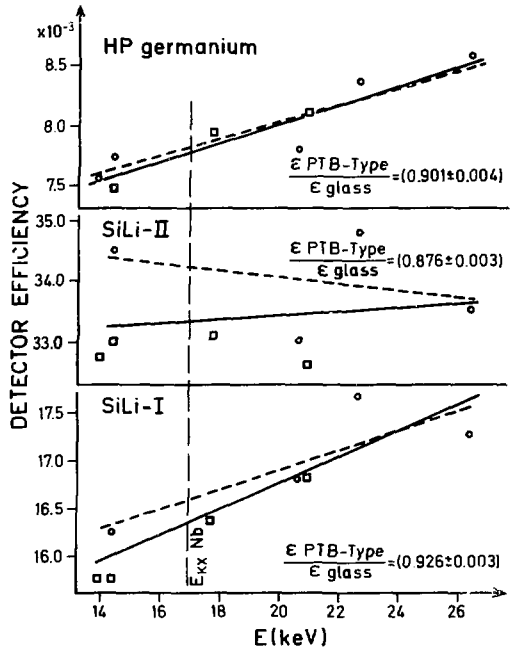

Fig. 2.1 Detector efficiencies corrected for transmission
□ ^{57}Co (γ 14.4 keV), ^{241}Am (LX rays)
○ ^{88}Y, ^{103}Ru and ^{109}Cd (KX rays), ^{241}Am (γ 26.35 keV)
—— *Linear regression through all points* (□ and ○)
--- *Linear regression through* ○ *points*

The PTB-type $^{93}Nb^{m}$ source 389-80 was then remeasured using the three detectors. The results of the measurements performed in 1980 on three sources on VYNS foils using the two SiLi detectors were now calculated with the re-estimated efficiencies. The obtained KX-ray emission rates were combined with the disintegration rates, determined in 1980 using the liquid scintillation technique, in order to obtain the KX-ray emission probability. The results obtained for the different sources and detectors are given in Table 2.2.

Table 2.2 Results of the KX-ray emission probability determinations

Adopted efficiencies	KX-ray emission probability					
	VYNS Sources		PTB-type 389-80			Mean value and standard error
	SiLi-I	SiLi-II	SiLi-I	SiLi-II	HP-Ge	
(1)	0.1142	0.1156	0.1149	0.1160	0.1164	0.1154 ± 0.0004
(2)	0.1127	0.1131	0.1133	0.1131	0.1158	0.1136 ± 0.0006
(3)	0.1153	0.1129	0.1156	0.1122	0.1171	0.1146 ± 0.0009

The overall mean value is 0.115. The standard error is ± 0.4 %; the systematic uncertainty is estimated to be ± 3.7 %: about ± 2.5 % for the photon detection efficiencies and ± 1.2 % for the $^{93}Nb^{m}$ disintegration rates. The final result of P_{KX} = (0.115 ± 0.005) is not significantly different from our 1980 value of (0.116 ± 0.004).

These new measurements do not solve the discrepancy between the PTB and CBNM results. The discrepancy is likely due to the utilization of different calibration nuclides and different decay data. Furthermore, this investigation shows clearly that the accuracy of the decay data of several nuclides used for the calibration of detectors is not yet satisfactory.

Half life of excited nuclear levels

D. Mouchel, H.H. Hansen

The half life of the excited level at 482.2 keV in ^{181}Ta has been determined by the delayed-coincidence technique. Detectors (NaI(Tl) and/or Pilot U plastic scintillators) with fast-timing properties and a time-to-amplitude converter (TAC) were used in these experiments. Photons of 135.1 and 482.2 keV did respectively trigger the start and stop inputs of the TAC. From 25 independent runs a result of $T_{1/2}$ = (10.67 ± 0.05)ns has been obtained for the half life. The given uncertainty contains random and systematic components. The details of those experiments and their evaluation are described in an internal report (1).

Similar experiments have been performed for the half-life determination of the excited level at 615.3 keV in ^{181}Ta. The β^- decaying nuclide ^{181}Hf has

(1) **D. Mouchel, H.H. Hansen, The half life of the 482.2 keV level in ^{181}Ta, GE/R/RN/16/82**

been deposited onto thin VYNS foils. Delayed coincidences were recorded between the β^- particles feeding the level and several γ rays deexciting it. A conventional fast-slow coincidence system has been used in connection with a TAC of start-stop type. Two different detectors were taken: a plastic scintillator (Pilot U) in the start channel and a NaI(Tl) crystal in the stop channel.

In the μs time range the finally achievable accuracy on the half life depends very much on the ratio of true delayed to chance coincidences. In order to reduce as much as possible the chance coincidence rate the following measures have been taken into consideration simultaneously: low-background photomultipliers, wide solid-angle geometries, low-activity radioactive sources, and a careful energy selection of the photons and particles involved.

From 21 measurements a preliminary mean value of $T_{1/2}$ = 17.64 μs has been deduced having a standard deviation of $\pm$ 0.19 μs.

Decay of ^{133}Ba

H.H. Hansen, D. Mouchel, R. Vaninbroukx, W. Zehner

Measurements for the determination of the half life have been continued. The solid state detector used until now (Ge(Li), 18 cm^3) has been replaced (pure Ge, 65 cm^3) and simultaneously the electronic equipment has been modernized. By this an appreciable improvement of the detection efficiency, the γ-peak resolution and the stability of amplification could be realized. A series of γ-ray reference spectra (from ^{60}Co and ^{137}Cs) has been recorded in order to establish a correspondence between measurements made with the old spectrometer and the new one. The evaluation of 3 sets of spectra is in progress as well as that of 2 additional runs made with the NaI(Tl) spectrometer.

Internal conversion ratios in the decay of ^{192}Ir

H.H. Hansen, D. Mouchel

The evaluation of a series of internal conversion spectra following the decay of ^{192}Ir has been accomplished. The purpose of the measurements performed with a magnetic β spectrometer was to determine the internal conversion ratio R = K/LM+ for pure E2 transitions. Complementary to the study of ^{152}Eu (1)

---

(1) H.H. Hansen, D. Mouchel, K/LM+ Internal Conversion Ratios for Pure E2 Transitions in the Decay of ^{152}Eu, CBNM/RN/25/81

two transitions of 205.8 and 316.5 keV (both of $2^+ \rightarrow 0^+$ type) in the decay of ^{192}Ir have been investigated. From 6 experimental runs the following results have been obtained: R(206 keV) = 1.05 and R(317 keV) = 1.715. The standard deviations are about 1 % and 3 %, respectively. A comparison made with theoretical values deduced for pure E2 multipolarity from the most recent tabulations of internal conversion coefficients reveals a very satisfactory agreement in both cases. This is discussed in detail as well as the final uncertainty of the results with contributions from random and systematic effects in an internal report (1).

Decay of ^{224}Ra

G. Bortels, D. Reher, R. Vaninbroukx

A paper on the emission probabilities for the 5.449 MeV α particles and 241 keV γ rays in the ^{224}Ra - ^{220}Rn decay has been submitted to the Int. J. Appl. Radiat. Isot. for publication as part of the Proceedings of the ICRM Seminar on α-Spectrometry Techniques and Applications, Geel, 14 October 1981.
The paper has the following abstract:

"The emission probability P_{α_1} for the 5.449 MeV α particles, which in the decay of ^{224}Ra populate the 241 keV level in ^{220}Rn, was measured using ^{224}Ra sources produced by recoil implantation from ^{228}Th and Si-surface-barrier detectors. Additionally, the 241 keV γ-emission probability, $P_\gamma(241)$ was measured using ^{228}Th sources and a calibrated intrinsic Ge detector. A pair of deduced values, $P_\gamma(241)$, P_{α_1}, was obtained from the measured data of P_{α_1} and $P_\gamma(241)$, respectively. The weighted mean of the measured and deduced data yielded the results of $P_{\alpha_1} = 0.0507 \pm 0.0005$ and $P_\gamma(241) = 0.0400 \pm 0.0007$. The quoted overall uncertainties of the mean correspond to $\bar{a}$ 68 % confidence level."

Gamma-ray emission probabilities in the decay of ^{228}Th and its daughters

R. Vaninbroukx, H.H. Hansen

A paper has been submitted to the Int. J. Appl. Radiat. Isot. for publication. It has the following abstract:

---

(1) H.H. Hansen, D. Mouchel, K/LM+ Internal Conversion Ratios for Pure E2 Transitions in the Decay of ^{192}Ir, GE/R/RN/17/82

" Gamma-ray emission probabilities useful for the assessment of ^{232}Th and ^{232}U by γ-ray spectrometry have been determined very accurately. The results were deduced from γ-ray spectra measured with a Ge(Li) and a high-purity-Ge detector using sources of ^{228}Th that is part of the decay chain of ^{232}Th and ^{232}U."

Gamma-ray emission probabilities in the decay of ^{235}U and ^{231}Th

R. Vaninbroukx, B. Denecke

A paper has been published with the following abstract [1]:

" The emission probabilities for the most prominent γ-ray transitions in the energy range from 25 to 206 keV accompanying the decay of ^{235}U and its radioactive daughter ^{231}Th were determined using calibrated Si(Li) and high purity Ge detectors. The results are:
$P_\gamma(25.65) = (0.145 \pm 0.003)$, $P_\gamma(84.16) = (0.066 \pm 0.003)$,
$P_\gamma(143.8) = (0.109 \mp 0.002)$, $P_\gamma(163.4) = (0.050 \mp 0.001)$,
$P_\gamma(185.7) = (0.575 \mp 0.009)$, $P_\gamma(205.3) = (0.050 \mp 0.002)$.
The quoted uncertainties, corresponding to a 1σ confidence level, take into account random and systematic uncertainties."

Decay of ^{238}Pu

G. Bortels, B. Denecke, R. Vaninbroukx

Measurements of alpha- and photon emission probabilities in the ^{238}Pu - ^{234}U decay have been performed.

Alpha emission probabilities were determined from 19 measurements with Si-surface barrier detectors of respectively 25 and 50 mm^2 active area using ^{238}Pu sources produced by evaporation in vacuum. The resolution obtained was 12.4 keV FWHM for source-to-detector solid angles from 0.6 down to 0.034% of 4π sr. The total number of counts in the α spectra was typically $7 \cdot 10^6$; counting rates were between 15 and 170 per second. Sum effects from α particles and conversion electrons have been corrected for by linear extrapolation of the number of counts in the peaks to zero solid angle. Similar sources were used for the determination of photon-emission probabilities (LX and γ rays) in the energy range 10 - 160 keV. These measurements were performed with calibrated high purity Ge and Si(Li) detectors. The disintegration rates of the sources were determined by α counting using detectors with well defined low-geometry solid angles. The results are summarized in Table 2.3. Quoted are the overall uncertainties to the mean corresponding to a 1σ confidence level.

---

(1) R. Vaninbroukx, B. Denecke, Determination of Gamma-Ray Emission Probabilities in the Decay of ^{235}U and ^{231}Th, Nucl. Instr. Methods 193, 27 (1982)

Table 2.3 Alpha- and photon emission probabilities in the decay of ^{238}Pu

Level in ^{234}U	Corresponding E_α (MeV)	Corresponding E_γ (keV)	Emission probabilities	
			P_α	P_{photon}
296 keV	5.206	152.7	0.000030 ± 0.000001 *	$(9.3 \pm 0.1)10^{-6}$
143 keV	5.358	99.9	0.00105 ± 0.00004	$(7.3 \pm 0.1)10^{-5}$
43 keV	5.457	43.5	0.2898 ± 0.0010	$(3.96 \pm 0.10)10^{-4}$
ground state	5.499	----	0.7091 ± 0.0010	---
		U - LX rays		
		$\bar{E}$ = 11.6 keV L_ℓ		0.0026 ± 0.0001
		$\bar{E}$ = 13.6 keV L_α		0.0406 ± 0.0006
		$\bar{E}$ = 17.2 keV L_β		0.0585 ± 0.0009
		$\bar{E}$ = 20.2 keV L_γ		0.0138 ± 0.0002

* Value deduced from the γ-ray measurements and taking into account the theoretical conversion coefficient.

Decay of ^{241}Pu

P. De Bièvre, M. Gallet, R Werz

A paper on the results of the ^{241}Pu half-life determination by isotope mass spectrometry was submitted for publication [1]. It has the following abstract:

" The decrease of the $^{241}Pu/^{240}Pu$ ratio due to the decay of ^{241}Pu and of the ratio of isotope ratios $\frac{^{241}Pu/^{240}Pu}{^{240}Pu/^{239}Pu}$ was measured with high precision isotope mass spectrometry over a period of six years using a 93 % isotopically enriched sample. The resulting value for the ^{241}Pu half life is (14.33 ± 0.02)a." •

---

(1) P. De Bièvre, M. Gallet, R. Werz, A Determination of the ^{241}Pu Half Life of Highly Enriched ^{241}Pu by Isotope Mass Spectrometry, Int. J. Mass Spectrometry, submitted for publication

Decay of ^{241}Am

B. Denecke

Measurements have been started to determine the 60 keV γ-ray emission probability. From these measurements it turned out that thick insensitive layers are grown on the surface of the specially shaped open CsI(Tl) detectors. These dead layers result in absorption corrections for the 60 keV γ rays and decrease the final accuracy of the results.
To measure the counting efficiency of the detectors the surfaces of the CsI crystals were scanned with a scanning device using collimated beams of α particles of ^{148}Gd and X rays of ^{109}Cd. Furthermore, various methods were tried to clean the crystals and remove the dead layers to a thickness smaller than 1 mg cm^{-2}.

2.2 COMPILATIONS AND EVALUATIONS

Internal conversion data

H.H. Hansen

The compilation of internal conversion data for nuclides with $Z > 60$ has been closed by October 1982. The listing of these data is very much advanced and that of the corresponding references is completed; it comprises about 800 entries.
The work on the evaluation of internal conversion coefficients of some selected transitions has been continued. It is completed for transitions in the decay of ^{22}Na, ^{57}Co, and ^{60}Co and it is in progress for those in the decays of ^{137}Cs and ^{203}Hg.

Half lives of ^{237}Pu and ^{242}Cm

R. Vaninbroukx

As part of the CBNM contribution to the Coordinated Research Programme (CRP) on the Measurement and Evaluation of Transactinium Isotope Nuclear Data of the International Atomic Energy Agency (IAEA) the half lives of ^{237}Pu and ^{242}Cm have been evaluated. The measurements described in the literature have been reviewed and assessed and weighted-mean values have been deduced for both half lives.

The recommended values and their uncertainties on a 1σ confidence level are:

^{237}Pu : $T_{1/2}$ = (45.17 $\pm$ 0.06)d
^{242}Cm : $T_{1/2}$ = (162.94 $\pm$ 0.06)d

Evaluation of some ^{109}Cd decay data

D. Reher

An internal report has been written with the following abstract [1]:

" A compilation of ^{109}Cd decay data relevant to solid state detector efficiency calibration was the basis for a preliminary evaluation. The data concerned are the K-capture probability, the K-shell fluorescence yield, the K-shell and the total conversion coefficients. The KX-ray emission probability and the γ-ray emission probability can be deduced from these decay data.
The evaluation revealed significant differences between experiments and theory in the case of the total conversion coefficient and between two groups of experimental data in the case of the relative K-capture probability.
A study on the feasibility of further data measurements shows that the accuracy of the decay data can be improved by using the following techniques: 1) 4π pressurized proportional counting, 2) 4π-CsI counting, 3) β-spectrometry, 4) LEXES, the low energy X-ray and electron spectrometer, and 5) liquid scintillation."

Fluorescence yields

W. Bambynek

The evaluation of K-shell fluorescence yields published between 1972 and December 1982 is finished. About 90 new values have been found and evaluated. From the total number of about 400 published K-shell fluorescence yields about one quarter has been selected for the list of recommended values which will be compared with recent theories.

2.3 IMPROVEMENT OF MEASUREMENTS AND SOURCE PREPARATION TECHNIQUES

Comparison of activity measurements of a ^{133}Ba solution

D. Reher, E. Celen, R. Vaninbroukx

This comparison was organized by the Bureau International des Poids et Mesures (BIPM) on behalf of Section II (Mesures des Radionucléides) of the Comité consultatif pour les Etalons de Mesures des Rayonnements Ionisants (CCEMRI).

---

(1) D. Reher, Compilation and Evaluation of some ^{109}Cd Decay Data and Feasibility Study for their Data Measurements, GE/R/RN/03-82

It was the second forerunner of a large-scale comparison. AECL, BIPM, CBNM, LMRI, OMH and PTB were participating. The difficulties encountered with the first comparison in 1981 were reproduced in the comparison of this year (see previous reporting period). There is a much too large spread on the results (± 1.4 %) as is expected in this kind of comparison. Furthermore, a significant difference of nearly 2 % is observed between ionization chamber measurements on the closed ampoules and the measurements of sources prepared from the solution in these ampoules. A comparison of the results of the different participating laboratories is shown in Fig. 2.2. The inconsistency in the results could neither be explained by adsorption of ^{133}Ba at the walls nor by simple weighing errors. A large-scale comparison on ^{133}Ba activity measurements will be delayed until the problems encountered in the past are solved. A decision is expected to be taken on the meeting of Section II of CCEMRI in May 1983.

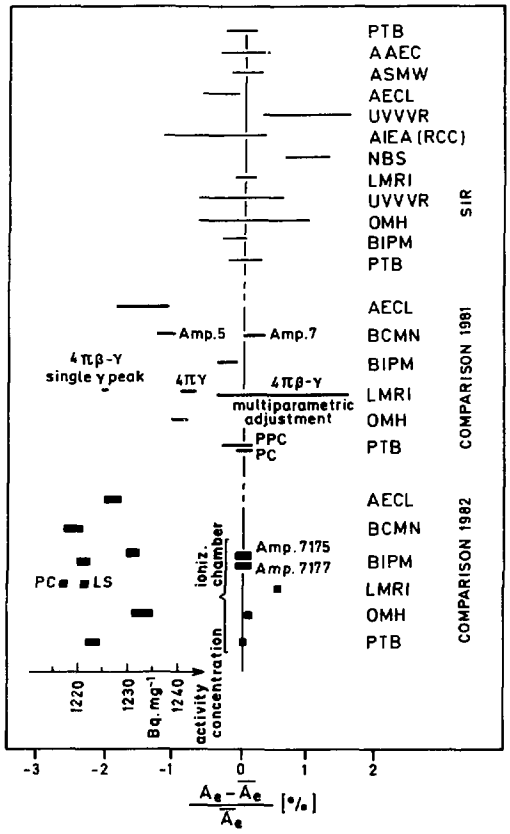

Fig. 2.2 Representation of the results of the ^{133}Ba intercomparisons (by courtesy of BIPM, Report BIPM-82/6). Both small scale intercomparisons were compared with the Système International de Référence (SIR) where closed standard ampoules were measured

Comparison of activity measurements of a ^{137}Cs solution

D. Reher, E. Celen, R. Vaninbroukx

This comparison was organized by the Bureau International des Poids et Mesures (BIPM) on behalf of Section II (Mesures des Radionucléides) of the Comité Consultatif pour les Etalons de Mesures des Rayonnements Ionisants (CCEMRI).

The objective of this comparison was to determine the activity concentration of a given ^{137}Cs solution using the $4\pi\beta$-γ efficiency tracer technique with ^{134}Cs as tracer.

Because of the half life (2.55 min) of the metastable state in the ^{137}Cs decay this radionuclide cannot be measured with the $4\pi\beta$-γ coincidence technique in the normal way. The variation of the β efficiency is controlled by the use of the tracer radionuclide ^{134}Cs which decays by prompt β-γ emission.

It was a large scale comparison with 18 laboratories participating. The solutions were distributed by PTB. CBNM received two solutions, 4 ml each of $^{137}CsCl$ and $^{134}CsCl$, respectively. The activity concentration of the ^{134}Cs solution was known, the latter being used as a tracer for the activity determination of the ^{137}Cs solution. Adsorption tests showed that less than $4 \cdot 10^{-4}$ of the total activity was adsorbed at the walls of the ampoules. Sources were prepared by dispensing a drop of each solution onto a VYNS foil (20 $\mu g\ cm^2$) coated on both sides with 15 $\mu g\ cm^2$ gold. Catanac was used as seeding agent. With these sources β efficiencies up to 93 % could be obtained. Measurements were carried out using both the γ counting method and the $4\pi\beta$-γ coincidence method. Although these two methods cannot be regarded as completely independent of each other, they are very valuable complementary methods, due to their different sensitivities to corrections. Fifteen sources were measured with the γ counting method in two different geometries. The result obtained was 604 $\pm$ 4 Bq mg^{-1}. The uncertainty contains 3 Bq mg^{-1} systematic and 1 Bq mg^{-1} statistical contributions at the level of one standard deviation.

From the same sources 13 were used in the $4\pi\beta$-γ coincidence method. Ten out of these 13 sources could

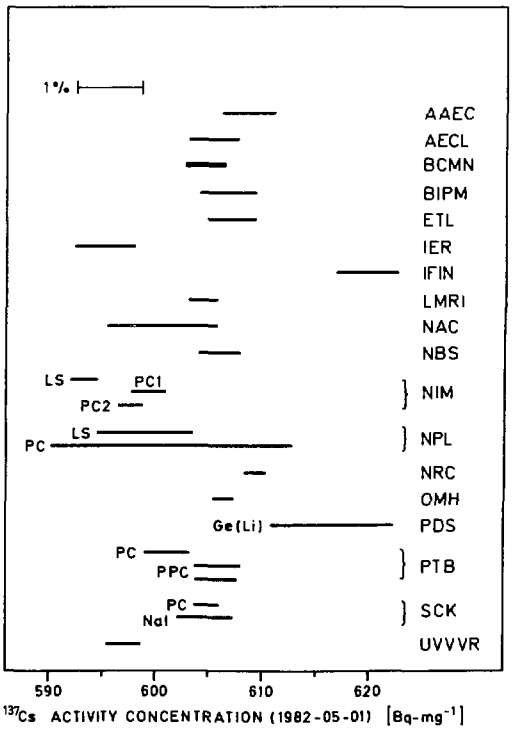

Fig. 2.3 Comparison of the results (by courtesy of BIPM, Report BIPM-82/14) of the full-scale ^{137}Cs international comparison

be used in the final result which was 604.5 ± 1.8 Bq mg^{-1}. The uncertainty is the square root of the sum of the squares of all uncertainty contributions to the final result.
This procedure had been suggested by BIPM. As can be seen from Fig. 2.3 the result is quite satisfactory.

Comparison of β^- spectra measurements with $^{90}Sr/Y$

H.H. Hansen

On the basis of a beta-ray spectrometry inquiry [1] performed in the frame of ICRM an intercomparison of $^{90}Sr/Y$ β^--spectra measurements has been initiated. The objective of this comparison is to determine the endpoint energies, spectrum shapes and relative intensities of the ^{90}Sr and ^{90}Y β^- spectra. To this purpose a series of β^--spectrum measurements have been made with the magnetic β spectrometer. Sources of different activity have been prepared by depositing a known amount of solution onto metal-coated VYNS foils. The number of electrons has been registered as a function of the electron momentum by measuring with small equal current increments. An example of such a spectrum is shown in Fig. 2.4a. Background spectra were obtained with the same sources screened from the spectrometer entrance by a 2 mm thick Cu disc. From the measured electron distributions corrected for background, scattering and resolution the shape factors have been determined. Both β^- spectra are 1st unique forbidden. The

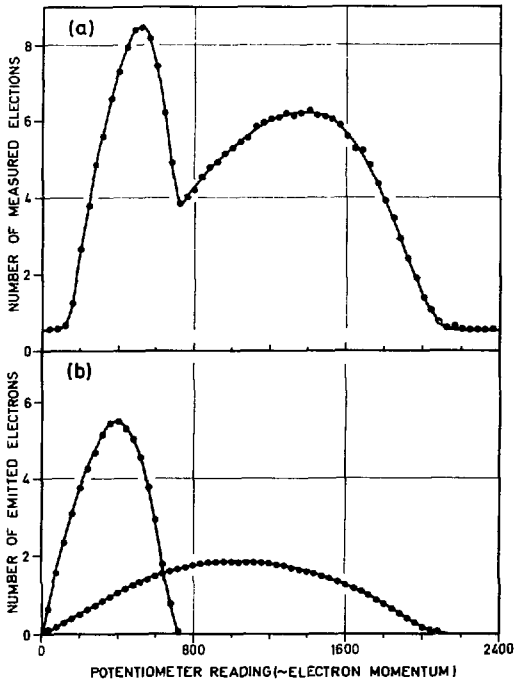

Fig. 2.4 Continuous spectra of $^{90}Sr/Y$. The number of electrons as measured with the magnetic β spectrometer (a) and as emitted from the $^{90}Sr/Y$ source (b) is plotted against the spectrometer's potentiometer reading (proportional to the electron momentum)

(1) P. Christmas, Beta-Ray Spectrometry Survey 1978, NPL Report RS 48 (1980)

correction factor to the theoretical shape has been expressed by $(1 + a\epsilon)$, with the electron energy ϵ in units of m_0c^2 and the correction coefficient a in units of $1/m_0c^2$.
From the Kurie plots the maximum β^- energies have been deduced as well as the emitted electron distribution (Fig. 2.4b).
Preliminary results obtained as mean values from 14 runs are summarized in Table 2.4. The quoted uncertainties are standard deviations.

Table 2.4 Results of $^{90}Sr/Y$ β spectra measurements

	$0^+ \rightarrow 2^-$ transition from ^{90}Sr decay	$2^- \rightarrow 0^+$ transition from ^{90}Y decay
max. β energy ϵ_o (m_0c^2) E_o (keV)	 2.068 ± 0.004 545.7 ± 1.1	 5.461 ± 0.003 2279.8 ± 1.3
shape factor	$C(\epsilon) \sim C_{theor}(\epsilon) \cdot C_{corr}(\epsilon)$ $C_{theor}(\epsilon) \sim (\epsilon_o-\epsilon)^2 + (\epsilon^2-1)$ $C_{corr}(\epsilon) \sim (1 + a\epsilon)$	
$a\left(\frac{1}{m_0c^2}\right)$	$-(0.03 \pm 0.01)$	$-(0.008 \pm 0.002)$

Measurement of electron capture nuclides by the $4\pi\beta$-γ coincidence technique

E. Funck*, A. Nylandsted Larsen**

A paper has been submitted to the Int. J. Appl. Radiat. Isot. for publication. It has the following abstract:

" The influence of low energy X rays and Auger electrons emitted by electron capture nuclides on $4\pi\beta$-γ coincidence measurements is investigated. Under the assumption that these radiations are not detected correction terms are developed for a number of nuclides that are in common use."

---

* Physikalisch-Technische Bundesanstalt, Braunschweig, GFR

** present address: Institute of Physics, University of Aarhus, Aarhus, Denmark

Counting of α particles under low geometry solid angle

B. Denecke

Absolute α-activity measurements are required as well for the determination of decay data as for mass assay of radioactive samples. The accuracy requested is 0.2 % and even better. At this accuracy level an accurate knowlegde of the solid angle and of the homogeneity of the radioactive material distributed over the source area is very important. Alpha-particle scattering and absorption effects lead to spectrum distortion in particular at low energies which must be determined correctly.

A Monte Carlo programme was developed to determine the correction for low-energy particle discrimination. Trajectories of α particles were simulated to start at random origin and direction within the source volume. The energy loss of these α particles was calculated, if they entered the solid angle of detection. Summing up all the "detected" particles and sorting them according to their final energy the simulated α spectrum could be built up. The ratio of the detected number to the total number of generated α particles is the solid angle of detection which is the major correction term in this counting method. The result of the Monte Carlo calculation of the solid angle was checked by a rapidly converging numerical integration algorithm. The code allows to calculate solid angles for a system of multiple spherical collimators mounted coaxially at planes parallel to the source plane. An excellent agreement was found between this and the Monte Carlo calculation. The latter will be refined by including scattering within the source, at the source backing and at the collimator edges. This will result in a more realistic approach for the spectrum shape calculations. Empirical corrections for self absorption and backscattering were determined experimentally for ^{232}Th fission-foil samples for counting in a 2π solid angle. This was achieved by comparison with results from counting at low (about 6 % of 4π) solid angle where those corrections are small.

A thesis on the numerical calculation of solid angles for complex source-detector arrangements has been presented and accepted by the Postuniversitair Centrum van de Universiteit Diepenbeek [1].

A scanning device was used to measure the activity distribution over the source area. With this distribution as weight function to correct for the source inhomogeneity the average solid angle of such an inhomogeneous source was calculated.

---

(1) B. Denecke, Numerieke berekening van ruimtehoeken voor complexe geometrische opstellingen van bron en detector in nucleaire metingen, Thesis 1982, Postuniversitair Centrum, Universiteit Diepenbeek, Belgium

Low-energy X-ray standards

W. Bambynek, G. Grosse, W. Oldenhof

The preparation of standardized X-ray sources for the calibration of Si(Li) detectors at energies below 4.5 keV has been continued.
Eight specimens of ^{55}Fe electroplated (Ø 5 mm) on stainless steel backings have been prepared. Their Mn KX-ray emission rates are between $2 \cdot 10^3$ and $1 \cdot 10^6$ s^{-1}. Covered with thin Al foils they will be used as sources for the fluorescence excitation of Al KX rays. Measurements with these sources have been performed to investigate the influence of the low-energy tailing of the Mn KX-ray line upon the Al KX-ray peak. For this purpose the above mentioned sources were measured without and with Al cover.
Fig. 2.5 shows two spectra normalized to the position and height of the Mn KX-ray peak. Spectrum A originates from an uncovered source and shows besides the 5.97 keV Mn KX-ray peak also the Mn LX-ray peak at 0.61 keV.
Spectrum B has been measured with the same source but covered with a 2.5 mg cm^{-2} thick Al foil. Besides the 5.97 keV Mn KX-ray peak it shows the Al KX-ray peak at 1.49 KeV caused by fluorescence excitation. The Mn LX rays are completely absorbed. From Fig. 2.5 it follows that the shapes of the Mn KX-ray peaks in both spectra A and B, are in excellent agreement for energies above about 2 keV. This allows to deduce a good correction for the tail of the Mn KX-ray peak under the Al KX-ray fluorescence peak which is one of the largest uncertainties in the standardization procedure of these sources.

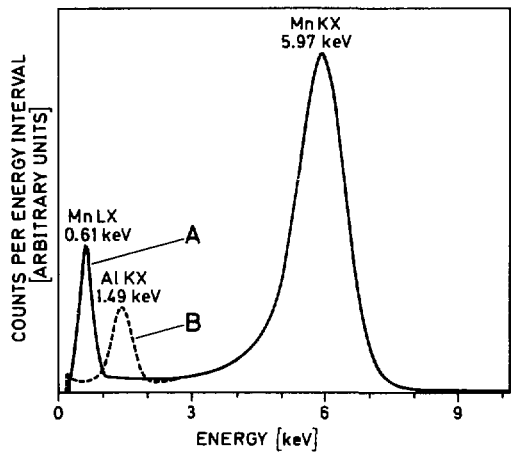

Fig. 2.5 Normalized spectra of an ^{55}Fe source on a stainless steel backing; A = uncovered, B = covered with a 2.5 mg cm^{-2} thick Al foil. Note that the shapes of the Mn KX-ray peaks in both spectra are identical above about 2 keV

In order to vary also the materials to be excited test experiments have been performed to produce Formvar foils with suspended phosphorus and sulfur, respectively. These tests were promising and will be pursued.

Preparation and characterization of thin $^{93}Nm^{m}$ sources

D. Reher, W. Oldenhof, I.V. Mitchell

A paper has been published with the following abstract [1]:

" A method is described for the preparation and characterization of sources of refractory metals. A focussed ion beam of small dimensions is used to produce thin, uniform and homogeneous radioactive deposits. The characteristics of these deposits have been compared with those of sources prepared by other methods. The influence of the type of backing has also been investigated. The following non-destructive techniques have been applied: Rutherford backscattering and particle induced X-ray emission, auto-radiography, and electron spectrometry. It is concluded that sources prepared by this technique are superior to those prepared by the more classical methods with respect to source purity and self-absorption."

Source preparation

W. Oldenhof, W. Zehner

The preparation of thin, homogeneous sources with low self and foil absorption is important for accurate measurements of low-energy X rays and electrons. The equipment to prepare thin sources by flash evaporation in vacuum is operational and has been used to prepare 55 sources.
The good results concerning the stability of carbon foils produced by sublimation have been confirmed. Fig. 2.6 shows an open ^{55}Fe source measured with a 4π proportional counter. The

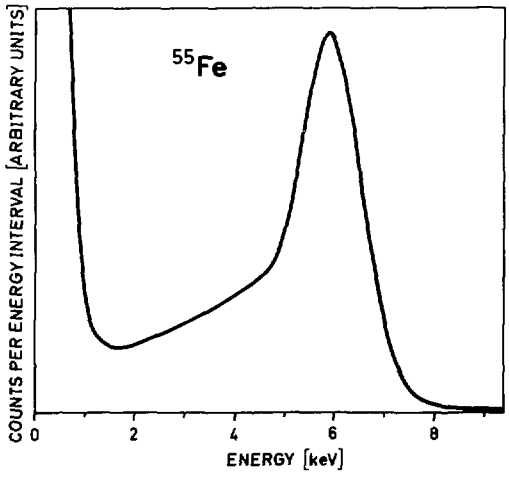

Fig. 2.6 K-Auger electron and KX-ray spectrum of an open ^{55}Fe source produced by Ar-ion bombardment onto a carbon foil of 20 $\mu g\ cm^{-2}$ thickness

(1) D. Reher, I.V. Mitchell, W. Oldenhof, The Preparation and Characterization of Radioactive Sources of Refractory Metals for Low Energy X-ray and Electron Spectrometry, Nucl. Inst. Methods 193, 191 (1982)

source was produced by bombardment of electrolyzed ^{55}Fe with an Ar-ion beam onto a carbon backing of 20 $\mu g\ cm^{-2}$ thickness. The relatively low tail of the Auger electrons which are very sensitive to self absorption indicates the quality of the source.
Various techniques were used for the preparation of about 180 radioactive sources on VYNS, Formvar and carbon backings, and about 370 supporting foils (VYNS, Formvar and carbon) were made.

Calibration service

G. Bortels, B. Denecke, R. Vaninbroukx

Sources and samples of ^{22}Na, ^{41}Ca, ^{55}Fe, ^{57}Co, ^{148}Gd, ^{232}Th, ^{235}U, ^{237}Np, ^{239}Pu, ^{240}Pu, ^{241}Am and ^{243}Am were standardized for various services inside CBNM and for the JRC Ispra, Jansen Pharmaceutica, Universities Gent and Frankfurt.

Radionuclides Group Data Acquisition System

D. Reher, A.B. Idzerda

A thesis on the development of the Radionuclides Group Data Acquisition System (RNDAS) has been presented to and accepted by the Postuniversitair Centrum of the University of Diepenbeek [(1)].
The system analysis for phase III of RNDAS is terminated. The purpose of the system is to control the experiments, to collect the measured data and to compute results from these data. RNDAS is a small hierarchical local star network of distributed intelligence. Its concept is shown in Fig. 2.7. At the level of the experiments we have installed intelligent CAMAC systems (see previous reporting period, phase II) which control the experiments and do the data acquisition. At the star-centre we have a minicomputer (PDP 11/34, phase I) which will be used for the mass storage of the data and the data processing. The links between the intelligent subsystems and the minicomputer are mainly to be used for data traffic, but they are not necessary for the functioning of the experiments and the system. Since no connections are foreseen between experiments these cannot disturb each other. In case of malfunction of the subsystem-to-minicomputer links data can be exchanged by

(1) D. Reher, RNDAS, een computersysteem voor de gegevensverzameling en de gegevensverwerking in de radionuclidenmetrologie, Thesis, 1982, Post-universitair Centrum, Universiteit Diepenbeek, Belgium

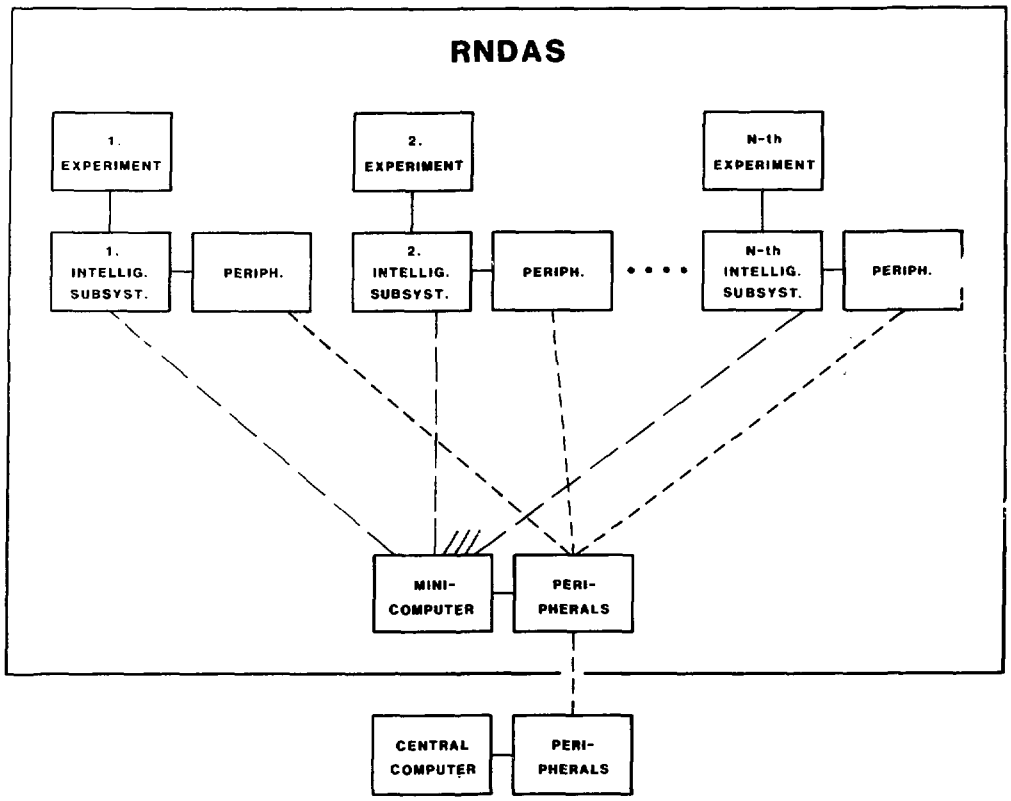

Fig. 2.7 The concept of RNDAS

use of compatible mass storage media such as floppy discs or magnetic tapes. For the implementation of phase III we want to approach the concept as far as possible, but on the other hand we have to obey a reasonable cost-benefit ratio which asks for certain compromises. It is, for example, not acceptable that an intelligent CAMAC system controls only one multichannel analyzer. For the same reason we will control two experiments by one CAMAC system, but only where one operator is responsible for both experiments. The configuration of phase III of RNDAS resulting from the system analysis is shown in Fig. 2.8.

Where scalers and multichannel analyzers and possibly other instruments have to be controlled simultaneously intelligent CAMAC systems are used. Stand-alone multichannel analyzers, which nowadays are intelligent on their own, are connected through CAMAC to an LSI 11/02 microcomputer which is entirely

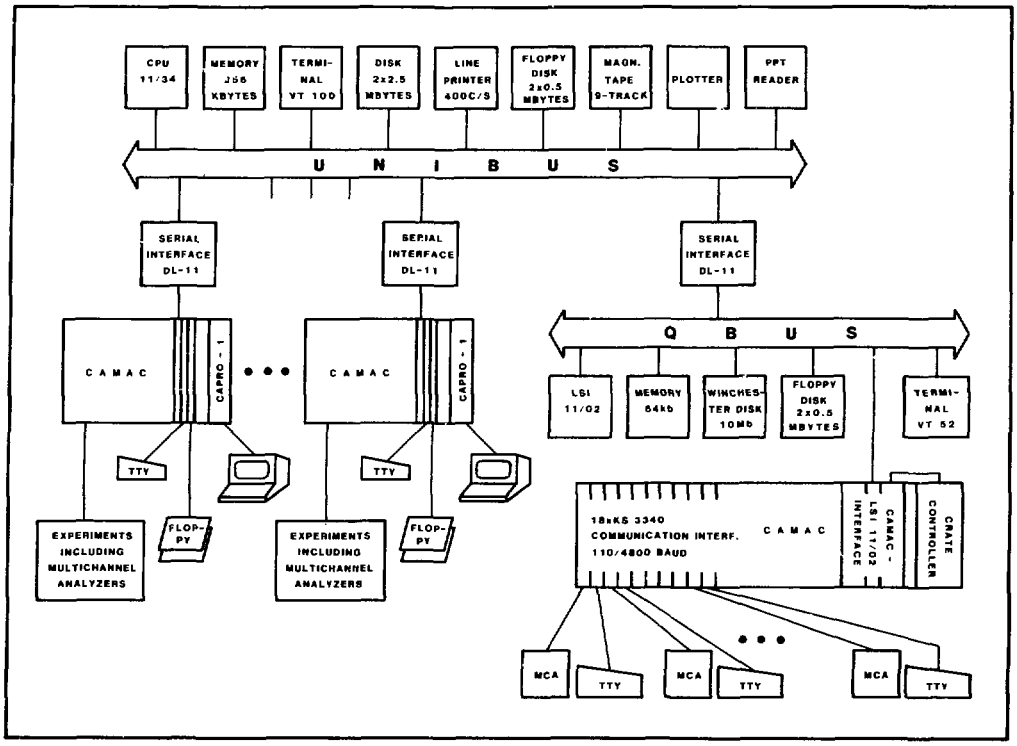

Fig. 2.8 Phase III of RNDAS

software compatible with the PDP 11/34. The PDP 11/34 computer is now completely free from control duties and is only used for data processing. Phase III of RNDAS is being installed in two steps, i.e. phase IIIa and phase IIIb, and is mainly constructed from the existing hardware and software of the phases I and II. For phase IIIa an LSI 11/02 microcomputer and a winchester disk has been installed to control the stand-alone multichannel analyzers, whereas with phase IIIb the intelligent CAMAC systems will be connected to the PDP 11/34 by means of serial links. A serial link between the PDP 11/34 and the LSI 11/2 was installed and is used for file transfer between the peripheries of both systems.

Although phase III of RNDAS is a compromise with the ideal concept of a hierarchical tree- or star-network of independent and distributed intelligence, this system has conserved its most important properties, which are:

- high degree of independence of experiments from each other,
- no system must rely on a link to the minicomputer,
- compatible floppy disks assure the exchange of data in case a link is down,
- the PDP 11/34 is capable of doing all the routine data processing work.

Phase IIIb is planned to be installed during the next reporting period.

LIST OF PUBLICATIONS

TOPICAL REPORTS

BAMBYNEK, W. - Decay data measured at CBNM since 1968. Nuclear Data for the Efficiency Calibration of Germanium Spectrometer Systems, edited by D.D. Hoppes and F.J. Schima, NBS-SPECIAL PUBLICATION 626 (1982) p. 33

REHER, D. - RNDAS, een computersysteem voor de gegevensverzameling en de gegevensverwerking in de radionucliden metrologie - Master thesis - Postuniversitair Centrum, Diepenbeek, 1982.

DENECKE, B. - Numerieke berekening van ruimtehoeken voor complexe geometrische opstellingen van bron en detector in nucleaire metingen - Master thesis - Postuniversitair Centrum, Diepenbeek, 1982

SMITH, D.L., LISKIEN, H. - Error analysis for the calculated spectrum-average cross section ratio of $^{63}Cu(n,\alpha)^{60}Co$ - to - $^{27}Al(n,\alpha)^{24}Na$ in a thick target $^{9}Be(d,n)^{10}B$ spectrum - EUR 8253 EN - European Applied Research Reports 4 (1982) 969

MEADOWS, J.W., BUDTZ-JØRGENSEN, C. - The fission fragment angular distributions and total kinetic energies for $^{235}U(n,f)$ from 0.18 to 8.83 MeV - Argonne National Laboratory Nuclear Data and Measurements Series ANL/NDM - 64 (1982)

PAUWELS, J., WESENBEEK, J., PAUWELS, M., VAN GESTEL, J. - The use of a visible light spectrophotometer for nuclear target production control - EUR 7985 EN

MAST, H., PAUWELS, J. - The preparation of a special target for induced and spontaneous fission studies - Newsletter of the INTDS - June 1982, Editor: CBNM

BATCHELOR, R. - 1981 Annual Status Report Nuclear Measurements - EUR 7918 EN

LE DUIGOU, Y. - Certification of a uranium metal reference material for chemical analyses - EUR 8349 EN

BOCKHOFF, K.H. - Nuclear Data for Science and Technology (Internat. Conf.) Antwerpen, 6-10 September 1982, Proceedings of the Conference, Reidel Publishing Company, Dordrecht, NL - EUR 8355 EN ISB 9027715602

ESCHBACH, H.L. - Intercomparison of Vacuum Measurement with an ionization gauge in the range of 10^{-4} Pa to 10^{-1} Pa - EUR 8312 EN (1982)

LE DUIGOU, Y. - Certification of a uranium metal reference material for chemical analyses - EUR 8349 EN (1982)

ROSSI, G., VAN AUDENHOVE, J., HAEMERS, L. - The preparation and certification of six reference materials for Zn in Zn ore concentrates - EUR 7430 EN

CONTRIBUTIONS TO CONFERENCES

BASTIAN, C. - Interactive design of neutron beam collimators using the Monte Carlo technique in APL - APL-82 - APL-Club of Germany - Deutsche Krebsforschung Heidelberg, 26-30/7/1982 - ORA 30311

WERZ, R., DE BIEVRE, P. - How enriched must enriched isotopes be to prepare accurate synthetic isotopic mixtures - 9th Int. Mass Spectrom. Conf., Vienna, 30.8 - 3.9.1982 - ORA 30318

DE BIEVRE, P. - Interlaboratory programmes: what do they do for us ? - ESARDA Specialists' Meeting, Petten, 27- 29 April 1982 - ORA 30367

DE BIEVRE, P., MEYER, H., VAN AUDENHOVE, J., CARPENTER, B.S., GRAMLICH, J.W. - Progress Report on the Establishment of U Isotope Abundance RM's for NDA - Ibid. - ORA 30445

VERDINGH, V., LE DUIGOU, Y. - Uranium metal RM EC N° 102; a European Community Reference Material for the elemental analysis of uranium - Ibid. - ORA 30466

KITCHIN, H.D., SALOME, J.M. - Thyratron Switch Generation of Multi-Kilovolt Pulses in the Nanoseconds Region for Linac Electron Gun Drive - 15th Power Modulator Symp. Hyatt Regency Baltimore, Baltimore, Maryland, USA, 14-16 June 1982 - ORA 30376

WAGEMANS, C., DERUYTTER, A.J. - Neutron Induced Fission Cross-Sections and Westcott g_f- factors for the Common Fissile Isotopes - 50th Anniversary of the Neutron, Cambridge, UK, 13-17 September 1982 - ORA 30414

MICHIELS, E., DE BIEVRE, P. - Accurate Isotope Dilution Mass Spectrometry of Li - 9th Internat. Mass Spectrometry Conf. Austrian MS Society, Wien, 30.8 - 3.9.1982 - ORA 30494

ROHR, G., BASTIAN, C., CORNELIS, E., SHELLEY, R., VAN DER VEEN, T. - Average Capture Cross Section of the Fission Product Nuclei ^{105}Pd and ^{108}Pd - NEANDC/NEACRP Spec. Meeting on Fast Neutron Capture Cross Sections, Argonne, 20-23 April 1982 - ORA 30474

CORVI, F. - Status of Neutron Capture Data of ^{233}U, ^{235}U and ^{239}Pu in the unresolved resonance region - Ibid. - ORA 30475

CORVI, F., MERLA, M., VAN DER VEEN, T., CALABRETTA, L. - Measurement of Neutron Capture Cross Section and Alpha of Physics ^{235}U from 2 to 85 keV - Ibid. - ORA 30476

ROHR, G. - The Status of Structural Material Data in the Resolved Resonance Region - Ibid. - ORA 30575

WAGEMANS, C., DERUYTTER, A.J. - The ^{241}Pu(n,f) cross-section and its normalization - Int. Conf. on Nucl. Data for Science and Technology, Antwerp, 6-10 Sept. 1982 - D. Reidel Publishing Cy., Dordrecht - The Netherlands, April 1983 - EUR 8355 EN - p. 69 - ORA 30602

MOORE, M.S., OLSEN, C.E., BUDTZ-JØRGENSEN, C., KNITTER, H.-H, WARTENA, J.A., WEIGMANN, H. - Neutron Induced Fission Cross Section of ^{244}Pu - Ibid. - p. 74 - ORA 30576

BRUSEGAN, A., CORVI, F., ALLEN, B.J., ROHR, G., SHELLEY, R., VAN DER VEEN, T., VAN DER VORST, C. - ^{54}Fe Neutron Capture Cross-Section - Ibid. - p. 127 - ORA 30658

CORVI, F., BRUSEGAN, A., BUYL, R., ROHR, G., SHELLEY, R., VAN DER VEEN, T. - High Resolution Neutron Capture Cross-Section of ^{56}Fe - Ibid. - p. 131 ORA 30659

ROHR, G., BRUSEGAN, A., CORVI, F., SHELLEY, R., VAN DER VEEN, T., VAN DER VORST, C. - Resonance Parameters of ^{57}Fe - Ibid. - p. 139 - ORA 30660

WATTECAMPS, E., LISKIEN, H., ARNOTTE, F. - Measurement of n,α cross sections for Cr, Fe and Ni at 14 MeV neutron energy - Ibid. - p. 156 - ORA 30663

WATTECAMPS, E., BABELIOWSKY, T., DE RAEDT, C., DE REGGE, P. - Reactor irradiations of ^{242}Pu, comparison of measured and calculated yields of ^{244}Pu, ^{243}Am and ^{244}Cm, and study of the fission product yields - Ibid. - p. 185 - ORA 30662

BUDTZ-JØRGENSEN, C., KNITTER, H.-H., SMITH, D.L. - Neutron induced fission cross section of ^{238}Pu in the energy range from 5 eV to 10 MeV - Ibid. - p. 206 - ORA 30665

CORNELIS, E., BASTIAN, C., ROHR, G., SHELLEY, R., VAN DER VEEN, T., VANPRAET, G. - Average Capture Cross Section of the Fission Product Nuclei ^{104,105,106,108,110}Pd - Ibid. - p. 222 - ORA 30657

LISKIEN, H., WOLFLE, R., QAIM, S. - Determination of ^{7}Li(n,n't)^{4}He cross sections - Ibid. - p. 349 - ORA 30661

WINKLER, G., PAVLIK, A., VONACH, H., PAULSEN, A., LISKIEN, H. - Precise Measurement of Cross Sections for the Reactions ^{90}Zr(n,2n)^{89}Zr and ^{58}Ni(n,2n)^{57}Ni from threshold to 20 MeV - Ibid. - p. 400 - ORA 30656

LISKIEN, H., SMITH, D.L., WIDERA, R. - The Spectrum-average cross section ratio of ^{63}Cu(n,α)^{60}Co-to-^{27}Al(n,α)^{24}Na in a thin-target ^{9}Be(d,n)^{10}B neutron spectrum - Ibid. - p. 409 - ORA 30605

KNITTER, H.-H., BUDTZ-JØRGENSEN, C., SMITH, D.L. - Determination of the ^{6}Li(n,t)^{4}He standard cross section - Ibid. - p. 451 - ORA 30606

ALLAERT, E., WAGEMANS, C., WEGENER-PENNING, G., DERUYTTER, A.J., BARTHELEMY, R. - Energy and Mass Distributions for ^{241}Pu(n_{th},f), ^{242}Pu(s.f.) and ^{244}Pu(s.f.)-fragments - Ibid. - p. 737 - ORA 30603

MEADOWS, J.W., BUDTZ-JØRGENSEN, C. - Fission fragment angular distribution and total kinetic energies for ^{235}U(n,f) - Ibid. - p. 740 - ORA 30586

KNITTER, H.-H., BUDTZ-JØRGENSEN, C. - Barrier height of Pu isotopes from (n,n'f)-thresholds - Ibid. - p. 744 - ORA 30664

JUNGMANN, C.R., WEIGMANN, H., MEWISSEN, L., POORTMANS, F., CORNELIS, E., THEOBALD, J.P. - Resonance structure of ^{32}S+n from Transmission and Differential Elastic Scattering Experiments - Ibid. - p. 777

WEIGMANN, H., AUCHAMPAUGH, G.F., LISOWSKI, P.W., MOORE, M.S., MORGAN, G.L. - Neutron induced charged particle reactions on ^{23}Na - Ibid. - p. 814 - ORA 30667

CRAMETZ, A., KNITTER, H.-H., SMITH, D.L. - Thick-target $^{9}Be(d,n)^{10}B$ neutron spectrum at $E_d \leq 7$ MeV - Ibid. - p. 902 - ORA 30604

VAN AUDENHOVE, J., COPPIETERS, L. - Further development of a piezoelectric jet device for the preparation of targets - World Conf. of Intern. Nucl. Target Development Soc., Seattle, 5-8 October 1982 - Nuclear Instruments and Methods, Proceedings in Press - ORA 30666

WEIGMANN, H. - Deuteron Exchange Mechanism for $^{6}Li(n,\alpha)$ - Nuclear Theory for Applications, Trieste, 12.9 - 23.10.1982 - ORA 30668

DE RAS, E. - Comments on the CBNM results of the photon dosimeter intercomparison (1981/82) organized by the Health and Safety Directorate V/E/3 of the Commission of the European Communities - 4th Info. Seminar on the European Radiation Prot. Dosimeter Intercomp. Prog., Bilthoven, 25-27 October 1982 - ORA 30737

TOURWÉ, H., TAYLOR, W.H., REHER, D., LLORET, R., NOLTHENIUS, N.J., WILLE, P., SCHWEIGHOFER, R. - Niobium dosimetry intercomparison in EBR II and BR2 - Proceedings of the Fourth ASTM-EURATOM Symposium on Reactor Dosimetry, Radiation Metrology Techniques, Data Bases, and Standardization, National Bureau of Standards, Gaithersburg, Maryland, March 22-26, 1982 - edited by F.B.K. Kam (Oak Ridge National Laboratory, Oak Ridge, 1982) NUREG/CP-0029, Vol. 1, CONF-820 321/V1, p. 401 - ORA 30395

VERDINGH, V., LE DUIGOU, Y. - Uranium metal RM EC 101, a European community RM for elemental analysis of U - ESARDA Specialists Meeting, Petten - 27-29.4 (1982) - ORA 30466

ALLAERT, E., WAGEMANS, C., WEGENER-PENNING, G., DERUYTTER, A.J., BARTHELEMY, R. - Energie en Massadistributies voor de $^{241}Pu(n_{th},f)$, $^{242}Pu(s.f)$ en $^{244}Pu(s.f)$ fragmenten - Algemene Wetenschappelijke Vergadering van de Belgische Natuurkundige Vereniging - Mons 3-4/6/1982 - Samenvattingen van de Mededelingen - N.P.-21

SCIENTIFIC OR TECHNICAL ARTICLES

DONNELLY, S.E., BARFOOT, K.M., WEBB, R.P., BODART, F., WERZ, R. - Helium Ion Bombardment of Thin Aluminium Films - Thin Solid Films Elsevier Sequoia S.A., P.O. Box 851, CH-1001 LAUSANNE 1 - ART 24890

PAVLIK, A., WINKLER, G., VONACH, H., PAULSEN, A., LISKIEN, H. - Precise measurement of cross sections for the $^{90}Zr(n,2n)^{89}Zr$ reaction from threshold to 20 MeV - Journal of Physics G (Nuclear Physics) 8 (1982) 1283 - ART 24753

QAIM, S.M., WOLFLE, R., LISKIEN, H. - Excitation functions of (n,t) reactions on ^{27}Al, ^{59}Co, and ^{93}Nb - Physical Review C25 (1982) 203 - ART 24513

BUDTZ-JØRGENSEN, C., MEADOWS, J. - Angular distribution and total kinetic energy for $^{232}Th(n,f)$ - Lecture Notes in Physics 158 (1982) 111, Springer Verlag

BARFOOT, K.M., MITCHELL, I.V., ESCHBACH, H.L., GILBOY, W.B. - Experimental Deuteron-Induced K X-Ray Emission Cross-Sections - J. Phys. B. At. Mol. Phys. 15 (1982) L845-L850 - ART 24986

BARNES, I.L., MURPHY, T.J., MICHIELS, E. - Certification of Lead Concentration in Standard Reference Materials by Isotope Dilution Mass Spectrometry - published in J. Assoc. Off. Anal. Chem., Vol. 65, No. 4, 1982

VERLINDEN, J., GIJBELS, R., SILVESTER, H., DE BIEVRE, P. - SIMS Investigation on the Diffusion of Chromium, Iron and Molybdenum in Polycrystalline Rhenium - J. Microsc. Spectrosc. Electron., Vol. 7, 1982, 291-302 - ART 24891

KACPEREK, A., DENECKE, B., REHER, D., BAMBYNEK, W. - The standardization of X-ray sources below 4 keV - Nuclear Instruments and Methods, 192 (1982) 109 ART 24529

REHER, D., MITCHELL, I.V., OLDENHOF, W. - The preparation and characterization of radioactive sources of refractory metals for low energy X-ray and electron spectrometry - Nuclear Instruments and Methods 193 (1982) 27

VANINBROUKX, R., DENECKE, B. - Determination of gamma-ray emission probabilities in the decay of ^{235}U and ^{231}Th - Nuclear Instruments and Methods 193 (1982) 191

HANSEN, H.-H., MOUCHEL, D., NYLANDSTED LARSEN, A. - Half-life of the 37.1 keV level in ^{121}Sb - Zeitschrift für Physik A, 305 (1982) 347 - ART 24667

REHER, D. - The internal conversion in ^{93m}Nb - International Journal of Applied Radiation and Isotopes 33 (1982) 537 - ART 24562

BERTHELOT, Ch., ESCHBACH, H.L., VERDINGH, V - A method for the precise evaluation of interferences in 44 MeV-Bremsstrahlung activations - J. Radioanal. Chemistry 72 (1982) 697/714

ESCHBACH, H.L., MITCHELL, I.V., BERTHELOT, Ch., VERHEYEN, F. - Reference samples for analysis by photon activation and Rutherford backscattering - J. Radioanal. Chemistry 72 (1982) 725/731

BARFOOT, K.M., MITCHELL, I.V., ESCHBACH, H.L., GILBOY, W.B. - Experimental deuteron-induced K X-ray emission cross sections - J. Phys. B: At. Mol. Phys. 15 (1982) L845/L850 - ART 24986

MITCHELL, I.V., MAENHAUT, W., RAEMDONCK, H., BODART, F. - Characterization of implanted and evaporated layers by RBS analysis - Nucl. Instr. Meth. 197 (1982) 51/57

BASTIN, J., BOMANS, M., DUGAIN, F., MICHAUT, C., PUJADE-RENAUD, J.M., VAN AUDENHOVE, J. - Utilisation de matériaux de référence pour analyse commerciale de grande précision, Exemple de minerais concentrés de zinc, Partie II: Fabrication des Matériaux de Référence, Analusis, 1982, v. 10, n° 6, p. 253 - (Congrès 1980) - ART 19796

JUNGMANN, C.R., WEIGMANN, H., MEWISSEN, L., POORTMANS, F., CORNELIS, E., THEOBALD, J.P. - Resonance structure of ^{32}S+n from transmission and differential elastic scattering experiments - Nuclear Physics A386 (1982) 287 - ART 24674

ALLAERT, E., WAGEMANS, C., WEGENER-PENNING, G., DERUYTTER, A.J., BARTHELEMY, R. - Energy and Mass Distributions for ^{241}Pu(n_{th},f), ^{242}Pu(s.f) and ^{244}Pu(s.f) Fragments - Nuclear Physics A380 (1982) 61-71 - ART 24654

CINDA ENTRIES

ELEMENT S	ELEMENT A	QUANTITY	TYPE	ENERGY MIN	ENERGY MAX	DOCUMENTATION REF VOL PAGE	DATE	LAB	COMMENTS
LI	006	TOTAL	EXPT-PROG	80+4	30+6	INDC(EUR)17 30	283	GEL	KNITTER+FROM TOT AND OEL XSECT
LI	006	DIFF ELASTIC	EXPT-PROG	80+4	30+6	INDC(EUR)17 30	283	GEL	KNITTER+FROM TOT AND DEL XSECT
LI	006	N,TRITON	EXPT-PROG	10+1	33+5	INDC(EUR)17 30	283	GEL	KNITTER+ANGDIST
LI	006	N,TRITON	EXPT-PROG	80+4	50+5	INDC(EUR)17 30	283	GEL	KNITTER+FROM TOT AND DEL XSECT
LI	007	N,N TRITON	EXPT-PROG	TR	80+6	INDC(EUR)17 22	283	GEL	LISKIEN+COOP KFA JUELICH
LI	007	N,N TRITON	EXPT-PROG	13+7	16+7	INDC(EUR)17 22	283	GEL	LISKIEN+COOP KFA JUELICH
NA	023	N,PROTON	EXPT-PROG	50+6	11+7	INDC(EUR)17 33	283	GEL	WEIGMANN+TOF AT LANKL/WNR
NA	023	N,ALPHA	EXPT-PROG	50+6	11+7	INDC(EUR)17 33	283	GEL	WEIGMANN+TOF AT LANKL/WNR
S	032	RESON PARAMS	EXPT-PROG	18+5	17+6	INDC(EUR)17 33	283	GEL	JUNGMANN+LINAC TOF
S	033	N,ALPHA	EXPT-PROG	10+4	10+6	INDC(EUR)17 34	283	GEL	WAGEMANS+LINAC TOF
CR		N,ALPHA	EXPT-PROG	14+7		INDC(EUR)17 22	283	GEL	WATTECAMPS+
FE		N,ALPHA	EXPT-PROG	14+7		INDC(EUR)17 22	283	GEL	WATTECAMPS+
FE	054	N,GAMMA	REVW-PROG	10+0	10+5	INDC(EUR)17 20	283	GEL	ROHR.REVIEW PAPER
FE	054	N,GAMMA	EXPT-PROG	30+2	50+5	INDC(EUR)17 15	283	GEL	BRUSEGAN+
FE	056	N,GAMMA	REVW-PROG	10+0	10+5	INDC(EUR)17 20	283	GEL	ROHR.REVIEW PAPER
FE	056	N,GAMMA	EXPT-PROG	25-2	25+5	INDC(EUR)17 18	283	GEL	CORVI+HIGH RESOL MEAS REL TO AG/AU
FE	057	TOTAL	EXPT-PROG	60+2	15+5	INDC(EUR)17 19	283	GEL	BRUSEGAN+LINAC TOF
FE	057	N,GAMMA	REVW-PROG	10+0	10+5	INDC(EUR)17 20	283	GEL	ROHR.REVIEW PAPER
NI		N,ALPHA	EXPT-PROG	14+7		INDC(EUR)17 22	283	GEL	WATTECAMPS+
NI	058	N,2N	EXPT-PROG	TR	20+7	INDC(EUR)17 25	283	GEL	WINKLER+
CU	063	N,ALPHA	EXPT-PROG	14+7		INDC(EUR)17 24	283	GEL	LISKIEN+REL TO AL(N,A)
ZR	090	N,2N	EXPT-PROG	TR	20+7	INDC(EUR)17 25	283	GEL	WINKLER+
PD	104	N,GAMMA	EXPT-PROG	10+1	60+5	INDC(EUR)17 21	283	GEL	CORNELIS+AVERAGE CAPT XSECT
PD	105	N,GAMMA	EXPT-PROG	10+1	60+5	INDC(EUR)17 21	283	GEL	CORNELIS+AVERAGE CAPT XSECT
PD	106	N,GAMMA	EXPT-PROG	10+1	60+5	INDC(EUR)17 21	283	GEL	CORNELIS+AVERAGE CAPT XSECT
PD	108	N,GAMMA	EXPT-PROG	10+1	60+5	INDC(EUR)17 21	283	GEL	CORNELIS+AVERAGE CAPT XSECT
PD	110	N,GAMMA	EXPT-PROG	10+1	60+5	INDC(EUR)17 21	283	GEL	CORNELIS+AVERAGE CAPT XSECT
TH	232	FRAG SPECTRA	EXPT-PROG	15+6	18+6	INDC(EUR)17 34	283	GEL	MEADOWS+ANGDIST AND KIN ENERGY
U	233	N,FISSION	EXPT-PROG	10-3	15+0	INDC(EUR)17 4	283	GEL	WAGEMANS+TEST MEASUREM
U	233	N,FISSION	EXPT-PROG	10-2	10+5	INDC(EUR)17 3	283	GEL	WAGEMANS+REL TO B10(N,A)
U	233	ALPHA	REVW-PROG	10+3	10+5	INDC(EUR)17 3	283	GEL	CORVI.REVIEW PAPER
U	235	N,FISSION	EXPT-PROG	20+3	85+4	INDC(EUR)17 4	283	GEL	CORVI+
U	235	ALPHA	REVW-PROG	10+3	10+5	INDC(EUR)17 3	283	GEL	CORVI.REVIEW PAPER
U	235	ALPHA	EXPT-PROG	20+3	85+4	INDC(EUR)17 4	283	GEL	CORVI+
U	235	FRAG SPECTRA	EXPT-PROG	18+5	88+6	INDC(EUR)17 34	283	GEL	MEADOWS+ANGDIST AND KIN ENERGY
U	238	RESON PARAMS	EXPT-PROG	60+0	43+3	INDC(EUR)17 5	283	GEL	ROHR+P WAVE CONTAM IN S WAVE RESON
PU	238	N,FISSION	EVAL-PROG	50+6	80+6	INDC(EUR)17 35	283	GEL	KNITTER+BARRIER HEI SEC CHANCE FISS
PU	238	N,FISSION	EXPT-PROG	50+0	10+7	INDC(EUR)17 9	283	GEL	BUDTZ-JØRGENSEN+
PU	239	N,FISSION	EVAL-PROG	50+6	80+6	INDC(EUR)17 35	283	GEL	KNITTER+BARRIER HEI SEC CHANCE FISS
PU	239	ALPHA	REVW-PROG	10+3	10+5	INDC(EUR)17 3	283	GEL	CORVI.REVIEW PAPER
PU	239	FRAG SPECTRA	EXPT-PROG	25-2		INDC(EUR)17 10	283	GEL	ALLAERT+
PU	240	N,FISSION	EVAL-PROG	50+6	80+6	INDC(EUR)17 35	283	GEL	KNITTER+BARRIER HEI SEC CHANCE FISS
PU	240	FRAG SPECTRA	EXPT-PROG	SPON		INDC(EUR)17 10	283	GEL	ALLAERT+
PU	241	N,FISSION	EVAL-PROG	50+6	80+6	INDC(EUR)17 35	283	GEL	KNITTER+BARRIER HEI SEC CHANCE FISS
PU	241	N,FISSION	EXPT-PROG	10-2	10+5	INDC(EUR)17 3	283	GEL	WAGEMANS+REL TO B10(N,A)
PU	241	FRAG SPECTRA	EXPT-PROG	25-2		INDC(EUR)17 11	283	GEL	ALLAERT+
PU	242	N,FISSION	EVAL-PROG	50+6	80+6	INDC(EUR)17 35	283	GEL	KNITTER+BARRIER HEI SEC CHANCE FISS
PU	242	N,FISSION	EXPT-PROG	30+5	10+7	INDC(EUR)17 13	283	GEL	WARTENA+REL TO U235 FISS
PU	242	FRAG SPECTRA	EXPT-PROG	SPON		INDC(EUR)17 11	283	GEL	ALLAERT+
PU	244	N,FISSION	EVAL-PROG	50+6	80+6	INDC(EUR)17 35	283	GEL	KNITTER+BARRIER HEI SEC CHANCE FISS
PU	244	N,FISSION	EXPT-PROG		10+5	INDC(EUR)17 14	283	GEL	MOORE+SUB-BARRIER FISSION
PU	244	FRAG SPECTRA	EXPT-PROG	SPON		INDC(EUR)17 11	283	GEL	ALLAERT+
CF	252	FRAG SPECTRA	EXPT-PROG	SPON		INDC(EUR)17 36	283	GEL	STRAEDE+FRAG MASS DIST